

## Cyclopentadienylrhodium Coordination to Alkenylarenes

Hubert Wadepohl,\* Alexander Metz, and Hans Pritzkow<sup>[a]</sup>

**Abstract:** Photochemical reaction of  $[\text{Rh}(\eta\text{-C}_5\text{H}_5)(\text{C}_2\text{H}_4)_2]$  (**5**) with alkenyl benzene derivatives  $\text{PhC}(\text{R}^1)=\text{CHR}^2$  results in the formation of four types of cyclopentadienylrhodium complexes: the mononuclear ethylene  $\eta^2$ -alkenylbenzene complexes  $[\text{Rh}(\eta\text{-C}_5\text{H}_5)(\eta\text{-C}_2\text{H}_4)(\eta^2\text{-PhC}(\text{R}^1)=\text{CHR}^2))]$  **9a** ( $\text{R}^1=\text{H}$ ,  $\text{R}^2=\text{Ph}$ ), **9b** ( $\text{R}^1=\text{Ph}$ ,  $\text{R}^2=\text{H}$ ), **9c** ( $\text{R}^1=\text{CH}_3$ ,  $\text{R}^2=\text{H}$ ), the mononuclear  $\eta^4$ -alkenylbenzene complex  $[\text{Rh}(\eta\text{-C}_5\text{H}_5)\{\beta,\alpha,1,2\text{-}\eta\text{-C}_6\text{H}_5\text{C}(\text{Ph})=\text{CH}_2\}]$  (**10**), the dinuclear  $\mu\text{-}\eta^4\text{-}\eta^4$ -alkenylbenzene complex  $[\text{anti-}\{\text{Rh}(\eta\text{-C}_5\text{H}_5)\}_2\{\mu\text{-}\beta,\alpha,1,2\text{-}$

$\eta\text{-}3,4,5,6\text{-}\eta\text{-C}_6\text{H}_5\text{C}(\text{Ph})=\text{CH}_2\}]$  (**11**), and the dinuclear rhodaindenyl complexes  $[\text{Rh}(\eta\text{-C}_5\text{H}_5)\{1\text{-}3,8,9\text{-}\eta\text{-}\{1\text{-}(\eta\text{-C}_5\text{H}_5)\}\text{-}3\text{-R}^1\text{-}1\text{-rhodaindenyl}\}]$  **12a** ( $\text{R}^1=\text{Ph}$ ), **12b** ( $\text{R}^1=\text{CH}_3$ ). Reaction of **5** with triisopropenylbenzene gives the dinuclear complex  $[\{\text{Rh}(\eta\text{-C}_5\text{H}_5)\}_2(\mu\text{-}\beta,\alpha,1,2\text{-}\eta\text{-}\beta',\alpha',4,3\text{-}\eta\text{-C}_6\text{H}_3\{\text{C}(\text{CH}_3)=\text{CH}_2\}_3)]$  (**13**).

**Keywords:** C–H activation • cyclopentadienyl ligands • diene complexes • dinuclear complexes • rhodium

In the complexes **9**, only the olefinic side chain of the alkenylbenzene binds to the metal. In the complexes **10**, **11**, **12**, and **13**, an arene nucleus coordinates to rhodium as a 1,3-diene moiety (or part thereof). The rhodaindenyl complexes **12** result from C–H activation of the alkenylbenzene at the  $\beta$  and *ortho* positions. The crystal and molecular structures of **9a**, **9b**, **10**, **11**, and **12a**, **b** were determined. The role of **9–11** and **13** as models for intermediates during alkenylbenzene-assisted self-assembly of tricobalt clusters is discussed.

## Introduction

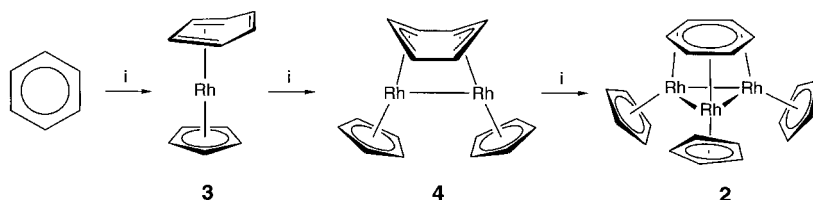
It has been demonstrated that metal cluster complexes with facial arene ligands  $[\text{M}(\eta\text{-C}_5\text{H}_5)_3(\mu_3\text{-arene})]$  **1** ( $\text{M}=\text{Co}$ ) and **2** ( $\text{M}=\text{Rh}$ ) can be obtained from the free arenes and sources that produce  $\{\text{M}(\eta\text{-C}_5\text{H}_5)\}$  fragments.<sup>[1]</sup> In such reactions, self-assembly of the trinuclear metal cluster is assisted by the arene ligand.<sup>[2]</sup> Benzene itself is only a suitable template for  $\text{M}=\text{Rh}$ . In this case, the reaction proceeds by consecutive addition of three  $\{\text{Rh}(\eta\text{-C}_5\text{H}_5)\}$  organometallic fragments to the benzene nucleus (Scheme 1).<sup>[3]</sup>

A mononuclear intermediate, complex **3**, was detected by mass spectroscopy. The structure of **3** was inferred by analogy

from the more stable iridium derivative.<sup>[4]</sup> The dinuclear intermediate **4** was isolated and unambiguously characterized by a crystal structure analysis. Unfortunately, the overall efficiency of the metal aggregation process is low, and complex **2** is formed in rather low yield.<sup>[3]</sup>

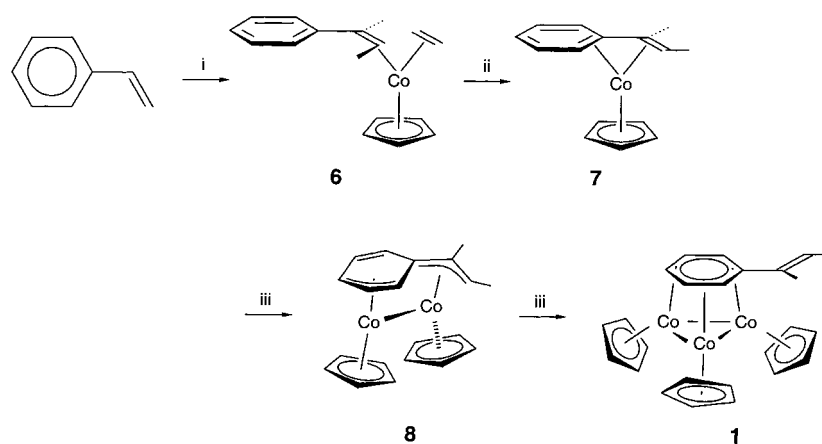
In marked contrast, reactive sources of the  $\{\text{Co}(\eta\text{-C}_5\text{H}_5)\}$  fragment do not undergo reaction with benzene or alkyl-substituted benzene derivatives. However, formation of the  $\mu_3$ -arene complexes **1** can be brought about by the use of arenes that carry an unsaturated (1-alkenyl) substituent.<sup>[5]</sup> In several cases, nearly quantitative yields of the cluster complexes **1** were obtained. A mechanism has been proposed which assigns a crucial role to the unsaturated side chain that guides the metal(s) to the arene ring (Scheme 2).<sup>[6]</sup> However, none of the proposed intermediates **6–8** have been directly observed or even isolated, and only a small number of reasonable models for them have been prepared.<sup>[5d, 6]</sup>

In the present work, we try to combine the merits of the  $\{\text{Rh}(\eta\text{-C}_5\text{H}_5)\}$  fragment with those of the alkenylbenzenes. It was our hope to find a more efficient synthetic pathway to  $\mu_3$ -arene trirhodium cluster complexes, and at the same time, more firmly establish some of the intermediates of the alkenylbenzene route.



Scheme 1. i) **5**,  $h\nu$ ,  $-2\text{C}_2\text{H}_4$ .

[a] Prof. Dr. H. Wadepohl, Dipl.-Chem. A. Metz, Dr. H. Pritzkow  
Anorganisch-Chemisches Institut der Ruprecht-Karls-Universität  
Im Neuenheimer Feld 270, 69120 Heidelberg (Germany)  
Fax: (+49) 6221-544197  
E-mail: bu9@ix.urz.uni-heidelberg.de



Scheme 2. i)  $[\text{Co}(\eta\text{-C}_5\text{H}_5)(\text{C}_2\text{H}_4)_2]$ ,  $-2\text{C}_2\text{H}_4$ ; ii)  $-\text{C}_2\text{H}_4$ ; iii)  $[\text{Co}(\eta\text{-C}_5\text{H}_5)(\text{C}_2\text{H}_4)_2]$ ,  $-2\text{C}_2\text{H}_4$ .

## Results

**Photochemical reactions of  $[\text{Rh}(\eta\text{-C}_5\text{H}_5)(\text{C}_2\text{H}_4)_2]$  (**5**) with 1-alkenylbenzenes  $\text{PhC}(\text{R}^1)=\text{CHR}^2$ :** The diethylene complex **5** was irradiated at low temperature in the presence of the alkenylbenzene derivatives  $\text{PhC}(\text{R}^1)=\text{CHR}^2$ : stilbene ( $\text{R}^1 = \text{H}$ ,  $\text{R}^2 = \text{Ph}$ ), 1,1-diphenylethylene ( $\text{R}^1 = \text{Ph}$ ,  $\text{R}^2 = \text{H}$ ) and  $\alpha$ -methylstyrene ( $\text{R}^1 = \text{Me}$ ,  $\text{R}^2 = \text{H}$ ). Details of the reaction conditions can be found in the Experimental Section. For reasons discussed below, the photochemical reactions were generally stopped when 40–50% of the ethylene complex **5** had been consumed. All yields are based on consumed starting material **5**. Workup of the reaction mixtures included chromatographic separation of the products on alumina, followed by recrystallization.

Four types of cyclopentadienylrhodium complexes were isolated: the mononuclear ethylene  $\eta^2$ -alkenylbenzene complexes **9**, the mononuclear  $\eta^4$ -alkenylbenzene complex **10**, the dinuclear  $\mu\text{-}\eta^4\text{:}\eta^4$ -alkenylbenzene complex **11**, and the dinuclear rhodaindenyl complexes **12**.

**Complexes of the type  $[\text{Rh}(\eta\text{-C}_5\text{H}_5)(\eta\text{-C}_2\text{H}_4)(\beta,\alpha\text{-}\eta\text{-alkenylbenzene})]$  (alkenylbenzene = *cis*-stilbene (**9a**), 1,1-diphenylethylene (**9b**), and  $\alpha$ -methylstyrene (**9c**)):** The complexes **9a**, **9b**, and **9c** were isolated as yellow crystalline solids in yields of 4, 14, and 28%, respectively. After irradiation of 1,1-diphenylethylene and **5** in *n*-hexane, complex **9b** was only detected in trace amounts, along with higher concentrations of  $[\text{Rh}(\eta\text{-C}_5\text{H}_5)(\eta^4\text{-1,1-diphenylethylene})]$  (**10**) and the dirhodium complex **12a** (vide infra). When the irradiation was performed in a mixture of *n*-hexane, diethyl ether, and acetonitrile, the main products were **9b** (14%) and  $[\{\text{Rh}(\eta\text{-C}_5\text{H}_5)\}_2(\mu\text{-1,1-diphenylethylene})]$  (**11**) (vide infra, 19%). Traces of **10** were also isolated from this mixture.

NMR spectroscopic data for the complexes **9** are given in Tables 1 and 2. When measured at ambient temperature, the ethylene ligand typically gave broad resonances in the  $^1\text{H}$  NMR spectra, which sharp-

ened on cooling. In the proton spectra of **9c**, two broad resonances are observed in the cyclopentadienyl region, along with numerous broad features with less intensity. Coalescence of the two  $\text{C}_5\text{H}_5$  signals occurred at  $27^\circ\text{C}$ ; further heating of the sample resulted in decomposition to give an insoluble brown solid. A well-resolved spectrum was obtained at 250 K (Table 1). Two sets of resonances for the  $\text{C}_5\text{H}_5$ ,  $\text{C}_2\text{H}_4$ , and  $\alpha$ -methylstyrene ligands are evident; they correspond to a mixture of two complexes

in a 3:2 ratio. The assignment of the signals to the various proton sites in the two species **A** and **B** (see Discussion below) was corroborated by  $^1\text{H}$  homonuclear correlation spectroscopy. The carbon resonances were assigned by means of the heteronuclear  $^1\text{H}/^{13}\text{C}$  correlated spectra (Table 2).

Single-crystal X-ray structure determinations were carried out for the complexes **9a** and **9b**. Selected bond lengths and angles are compiled in Table 3. Views of the molecules are depicted in Figures 1 and 2.

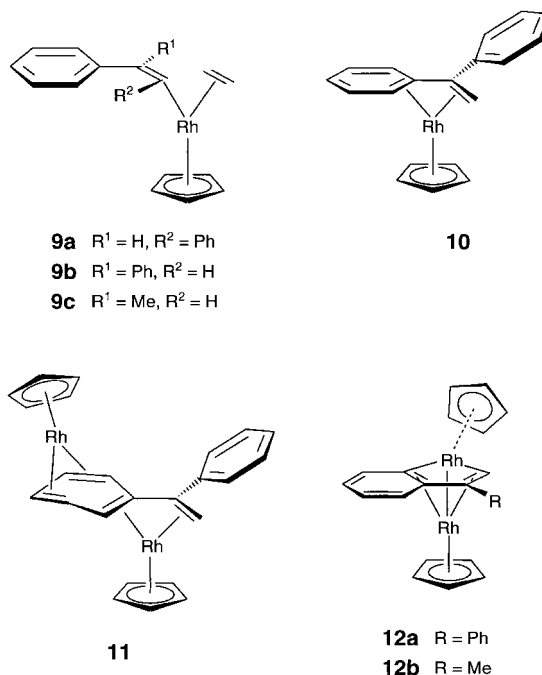


Table 1.  $^1\text{H}$  NMR spectroscopic data ( $\delta$ , multiplicity, intensity; in  $\text{C}_6\text{D}_6$ ) of complexes  $[\text{Rh}(\eta\text{-C}_5\text{H}_5)(\eta\text{-C}_2\text{H}_4)(\eta^2\text{-PhC}(\text{R}^1)=\text{CHR}^2)]$  **9**.

|                             | $\text{R}^1$ | $\text{R}^2$ | $\text{C}_5\text{H}_5$                                   | $\text{C}_2\text{H}_4$                                      | $\text{CR}^1\text{Ph}$  | $\text{CHR}^2$   |
|-----------------------------|--------------|--------------|--|---|---|--|
| <b>9a</b>                   | H            | Ph           | 4.54 (s, 5)  | 1.27 (m, 2), 3.02 (m) <sup>[a]</sup>                        | 7.05–7.41 (m, 10)   | 3.02 (m) <sup>[a]</sup>  |
| <b>9b</b> <sup>[b, c]</sup> | Ph           | H            | 4.39 (s, 5)  | 0.67 (m, 1), 1.12 (m, 1), 2.64 (m, 1), 2.89 (m, 1)          | 6.97–7.43 (m, 10)   | 2.22 (s, 1), 3.61 (s, 1)   |
| <b>9c</b> <sup>[c, d]</sup> | Me           | H            | 4.48 (d, 5) <sup>[e]</sup><br>4.82 (d, 5) <sup>[f]</sup> | 1.83 (m) <sup>[e, f]</sup><br>2.7–3.0 (m) <sup>[e, f]</sup> | 1.07 (d, 3), <sup>[e]</sup> 1.83 (s, 3) <sup>[f]</sup><br>6.9–7.3 (m) <sup>[e, f]</sup> | 1.35 (s, 1), <sup>[e]</sup> 3.97 (d, 1) <sup>[e]</sup><br>2.19 (d, 1), <sup>[f]</sup> 3.15 (d, 1) <sup>[f]</sup> |

[a] Overlapping resonances, total intensity = 4. [b] 216 K. [c] In  $[\text{D}_8]\text{toluene}$ . [d] 253 K. [e] Species **A**. [f] Species **B**.

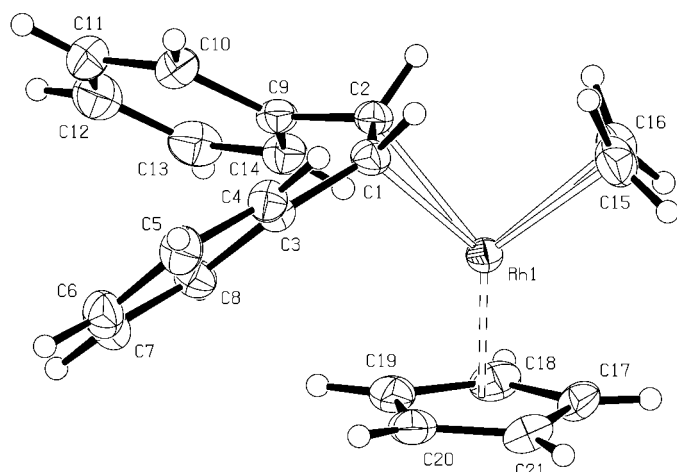
Table 2.  $^{13}\text{C}\{^1\text{H}\}$  NMR spectroscopic data ( $\delta$ ,  $J(\text{Rh},\text{C})$  [Hz] in parentheses;  $\text{C}_6\text{D}_6$ ) of complexes  $[\text{Rh}(\eta\text{-C}_5\text{H}_5)(\eta\text{-C}_2\text{H}_4)(\eta^2\text{-PhC(R}^1\text{)=CHR}^2)]$  **9**.

|                             | R <sup>1</sup> | R <sup>2</sup> | C <sub>5</sub> H <sub>5</sub>                          | C <sub>2</sub> H <sub>4</sub>  | CR <sup>1</sup> Ph  | CHR <sup>2</sup>   |
|-----------------------------|----------------|----------------|--|--|---|--|
| <b>9a</b>                   | H              | Ph             | 91.8 (4.2)   | 39.6 (13.2)  | 62.5 (13.2), 125.3, 127.7, 130.5, 145.3 <sup>[a]</sup>  |  |
| <b>9b</b> <sup>[b, c]</sup> | Ph             | H              | 90.2 (4.0)   | 37.8 (14.0), 42.3 (13.5)   | 72.2 (14.0), 125.3 <sup>[d]</sup> , 127.2 <sup>[d]</sup> , 127.9 <sup>[d]</sup> , 129.3 <sup>[d]</sup> , 130.4, 143.7 <sup>[a]</sup> , 150.2 <sup>[a]</sup> | 33.7 (13)  |
| <b>9c</b> <sup>[b, e]</sup> | Me             | H              | 90.6 (4.0) <sup>[f]</sup><br>89.2 (4.0) <sup>[g]</sup> | 36.3 (14) <sup>[f, h]</sup><br>34.4 (14) <sup>[g, h]</sup> , 37.4 (14) <sup>[g, h]</sup> | 151.9 (1.5) <sup>[f, i]</sup><br>146.6 (1.6) <sup>[g, i]</sup>  | 41.8 (14) <sup>[f, h]</sup><br>38.1 (14) <sup>[g, h]</sup> |

[a]  $C_{\text{ipso}}$ . [b] In  $[\text{D}_8]\text{toluene}$ . [c] 240 K. [d] Overlap with solvent resonances. [e] 253 K. [f] Species **A**. [g] Species **B**. [h] Tentative assignment of the methylene groups. [i]  $C_{\text{ipso}}$ : the phenyl CH resonances overlap with solvent signals.

Table 3. Selected bond lengths [ $\text{\AA}$ ] and angles [ $^\circ$ ] of complexes  $[\text{Rh}(\eta\text{-C}_5\text{H}_5)(\eta\text{-C}_2\text{H}_4)(\eta^2\text{-PhC(R}^1\text{)=CHR}^2)]$  **9a** and **9b**.

|                                   |                 | <b>9a</b>         |                 | <b>9b</b>         |
|-----------------------------------|-----------------|-------------------|-----------------|-------------------|
| ethylene                          | C15–C16         | 1.398(4)          | C3–C4           | 1.404(5)          |
|                                   | Rh1–C15         | 2.129(3)          | Rh1–C3          | 2.124(3)          |
|                                   | Rh1–C16         | 2.137(3)          | Rh1–C4          | 2.141(3)          |
| $\text{Ph}_2\text{C}_2\text{H}_2$ | C1–C2           | 1.431(3)          | C1–C2           | 1.421(4)          |
|                                   | Rh1–C1          | 2.174(2)          | Rh1–C1          | 2.103(3)          |
|                                   | Rh1–C2          | 2.134(2)          | Rh1–C2          | 2.182(3)          |
|                                   | C3–C1–C2        | 127.1(2)          | C1–C2–C5        | 119.5(2)          |
|                                   | C9–C2–C1        | 125.4(2)          | C1–C2–C11       | 117.9(2)          |
|                                   | C3–C1–C2–C9     | 6.6(4)            | C5–C2–C11       | 113.8(2)          |
| $\text{C}_5\text{H}_5$            | Rh–(C17 to C21) | 2.206(3)–2.285(2) | Rh–(C17 to C21) | 2.220(3)–2.286(3) |

Figure 1. Molecular structure of the complex  $[\text{Rh}(\eta\text{-C}_5\text{H}_5)(\eta\text{-C}_2\text{H}_4)(\eta^2\text{-Z-stilbene})]$  (**9a**).

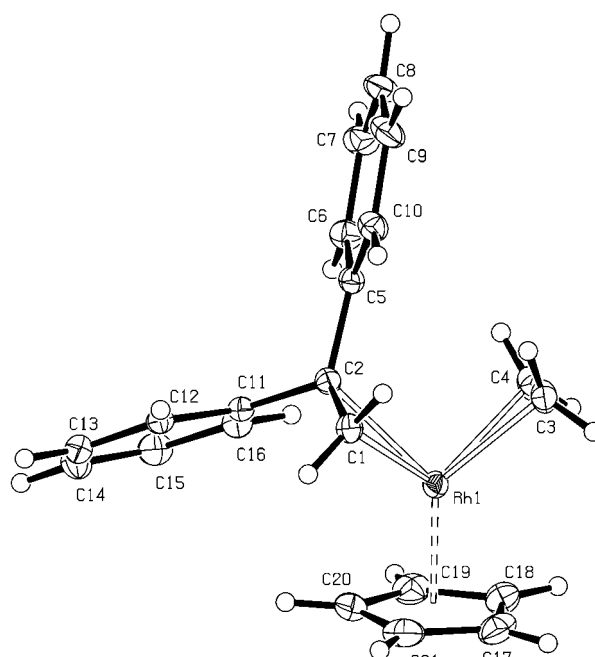
The complexes have an ethylene and a 1,2-diphenylethylene (**9a**) or 1,1-diphenylethylene (**9b**) ligand coordinated to a  $\{\text{Rh}(\eta\text{-C}_5\text{H}_5)\}$  moiety in a  $\eta^2$  fashion. The stilbene ligand in **9a** adopts the *Z* (*cis*) configuration. In both structures, the four carbon atoms of the two  $\eta^2$ -olefins are not in a plane. The (improper) torsion angles between the two coordinated C–C bonds are  $11^\circ$  in **9a** (C1–C2–C16–C15) and  $22^\circ$  in **9b** (C1–C2–C4–C3). The angle between the vectors which link the rhodium atom to the centers of the two  $\eta^2\text{-C}_2$  units are  $94^\circ$  (**9a**) and  $97^\circ$  (**9b**), respectively.

$[\text{Rh}(\eta\text{-C}_5\text{H}_5)\{\beta,\alpha,1,2\text{-}\eta\text{-}(\alpha\text{-phenylethylene})\}]$  (**10**): Complex **10** was obtained as red crystals in 8 % yield after irradiation of an equimolar mixture of **5** and 1,1-diphenylethylene in *n*-hexane/

diethyl ether. A second major product, the rhodaindenyl-cyclopentadienylrhodium complex **12a** (vide infra) was isolated in 16 % yield. Only traces of complex **9b** were separated from the reaction mixture. As mentioned above, **10** was also isolated in trace amounts when the photochemical reaction was carried out in the presence of acetonitrile.

The proton NMR spectrum of **10** exhibits two resonances (a multiplet at  $\delta = 0.59$  and a somewhat broadened singlet at  $\delta = 2.73$ ) from the *endo* and *exo* protons, respectively, of the methylene group of the 1,1-diphenylethylene ligand. A doublet at  $\delta = 3.11$  is caused by the proton on C2 of the phenyl ring which is partially coordinated to the metal. The other phenyl resonances appear as three groups of multiplets in the low-field region ( $6.6 \leq \delta \leq$

7.7) of the spectrum. The carbon NMR spectrum shows a similar pattern: resonances at higher field ( $\delta = 34.0$  ( $\text{CH}_2$ ), 59.3 (C2) and 83.9, 84.8 ( $C_{\text{ipso}}$  and  $C_\alpha$ ), all coupled to rhodium, and a total of eight singlets at lower field ( $121.5 \leq \delta \leq 141$ ), arising from the rest of the phenyl carbons.

Figure 2. Molecular structure of the complex  $[\text{Rh}(\eta\text{-C}_5\text{H}_5)(\eta\text{-C}_2\text{H}_4)(\eta^2\text{-1,1-diphenylethene})]$  (**9b**).

The molecular structure of **10** in the solid was elucidated by a crystal structure analysis (Figure 3), which unambiguously shows the  $\beta,\alpha,1,2-\eta^4$  coordination of the alkenylbenzene

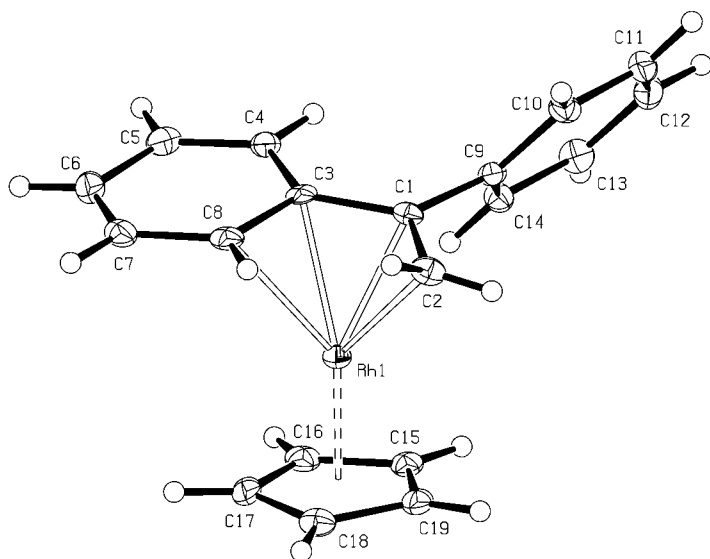


Figure 3. Molecular structure of the complex  $[\text{Rh}(\eta\text{-C}_5\text{H}_5)\{\beta,\alpha,1,2\text{-}\eta\text{-(}\alpha\text{-phenylstyrene)}\}]$  (**10**).

ligand to the  $\{\text{Rh}(\eta\text{-C}_5\text{H}_5)\}$  group. The metal-coordinated part of the  $\eta^4$ -ligand is essentially planar (root mean-square deviation from the best plane: 0.01 Å). The  $\eta^2$ -coordinated phenyl ring is also nearly planar (0.016 Å deviation); it is at an angle of 6.4° to the coordination plane, comprised of C2, C1, C3, and C8. Important bond lengths and angles are collected in Table 4.

$[\text{anti-}\{\text{Rh}(\eta\text{-C}_5\text{H}_5)\}_2\{\mu\text{-}\beta,\alpha,1,2\text{-}\eta\text{:}3,4,5,6\text{-}\eta\text{-(}\alpha\text{-phenylstyrene)}\}]$  (**11**): As mentioned above, this purple-blue complex was isolated in 19% yield following the irradiation of **5** and 1,1-diphenylethylene in a mixture of *n*-hexane, diethyl ether, and acetonitrile. Higher yields of **11** (45–55%) were obtained when **10** and a slight excess of **5** were irradiated in diethyl ether.

The NMR spectra of **11** exhibit a large number of resonances, both for  $^1\text{H}$  and  $^{13}\text{C}$ . The carbon spectrum shows three signals in the low-field region,  $127 \leq \delta \leq 141$ , that result

from the free phenyl group. All the other resonances are at higher field ( $32 \leq \delta \leq 102$ ) and coupled to rhodium. A similar pattern is shown in the proton spectrum: in addition to the resonances of a free phenyl substituent at  $\delta \approx 7.5$ , there are six multiplets in the range  $0.3 \leq \delta \leq 6$  for the other seven protons of the bridging alkenylbenzene ligand. The two cyclopentadienyl resonances are clearly separated in both the proton and carbon spectra.

The molecular structure of **11** was determined by crystal structure analysis (Figure 4). Important bond lengths and angles are given in Table 5. Two  $\{\text{Rh}(\eta\text{-C}_5\text{H}_5)\}$  groups are

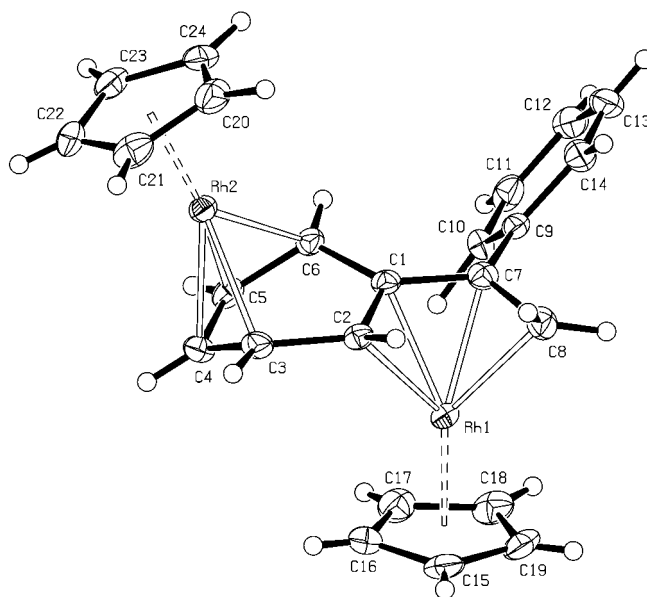


Figure 4. Molecular structure of the complex  $[\text{anti-}\{\text{Rh}(\eta\text{-C}_5\text{H}_5)\}_2\{\mu\text{-}\beta,\alpha,1,2\text{-}\eta\text{:}3,4,5,6\text{-}\eta\text{-(}\alpha\text{-phenylstyrene)}\}]$  (**11**).

bonded to a bridging  $\alpha$ -phenylstyrene ligand in an antifacial fashion. The bridging ligand is partitioned into two  $\eta^4$ -diene units (one consisting of the olefinic side chain, C1(*ipso*) and C2, the other comprised of the other four carbon atoms of the phenyl ring), each of which is coordinated to a  $\{\text{Rh}(\eta\text{-C}_5\text{H}_5)\}$  group. The two  $\eta^4$ -diene systems with internal C–C bond lengths ranging from 1.422 to 1.440 Å are fused together by two much longer bonds (1.478, 1.482 Å). The  $\eta^4$ -coordination planes are at an angle of 34°.

**Complexes of the type  $[\text{Rh}(\eta\text{-C}_5\text{H}_5)\{1\text{-}3,8,9\text{-}\eta\text{-(}\eta\text{-C}_5\text{H}_5\text{)}\}\text{-}3\text{-}R\text{-}1\text{-rhodaindenyl}]$  (**12a**:  $R = \text{Ph}$ , **12b**:  $R = \text{CH}_3$ ):** The rhodaindenylcyclopentadienylrhodium complexes **12a**, **b** were generated from **5** and 1,1-diphenylethylene or  $\alpha$ -methylstyrene in 18% and 8% yield, respectively. Compound **12a** was also formed when complex **9b** was irradiated in the presence of **5**. Quite significantly, an analogous reaction involving complexes **10** and **5**, or UV irradiation of complex **11** did not produce complex **12a**. In the proton NMR spectra of **12a**, all the resonances of the rhodaindenyl moiety are at rather low field, in the range  $6.7 \leq \delta \leq 8.2$ . The only ring proton of the metallacycle five-membered ring of this ligand resonates at particularly low field,  $\delta = 8.2$ . The carbon spectrum is quite complex because of the low symmetry of the complex and the

Table 4. Selected bond lengths [Å] and angles [°] of  $[\text{Rh}(\eta\text{-C}_5\text{H}_5)\{\beta,\alpha,1,2\text{-}\eta\text{-C}_6\text{H}_5\text{C(Ph)=CH}_2\}]$  (**10**).

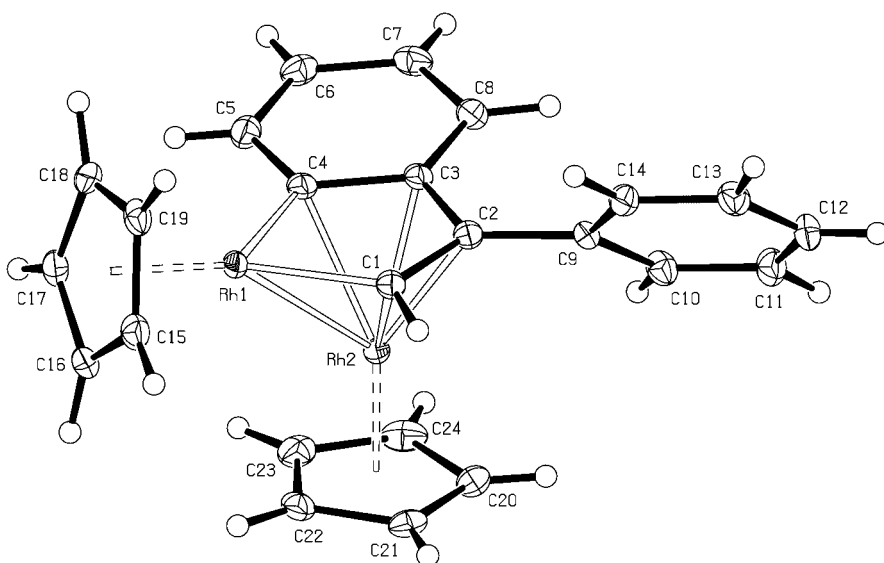
|                  |                   |          |          |
|------------------|-------------------|----------|----------|
| Rh1–C1           | 2.092(4)          | Rh1–C2   | 2.143(4) |
| Rh1–C3           | 2.173(5)          | Rh1–C8   | 2.247(4) |
| Rh1–(C15 to C19) | 2.182(4)–2.283(4) | C1–C2    | 1.448(5) |
| C1–C3            | 1.451(5)          | C1–C9    | 1.495(5) |
| C3–C8            | 1.442(5)          | C3–C4    | 1.440(5) |
| C4–C5            | 1.364(5)          | C5–C6    | 1.428(5) |
| C6–C7            | 1.354(6)          | C7–C8    | 1.442(6) |
| C2–C1–C3         | 116.5(3)          | C2–C1–C9 | 122.0(3) |
| C3–C1–C9         | 121.5(3)          | C1–C3–C8 | 116.4(3) |
| C1–C3–C4         | 124.6(3)          | C4–C3–C8 | 118.7(4) |
| C3–C4–C5         | 120.8(3)          | C4–C5–C6 | 120.8(4) |
| C5–C6–C7         | 120.0(4)          | C6–C7–C8 | 121.9(4) |
| C7–C8–C3         | 117.7(4)          |          |          |

Table 5. Selected bond lengths [Å] and angles [°] of complex  $[\text{anti-}[\text{Rh}(\eta\text{-C}_5\text{H}_5)]_2\{\mu\text{-}\beta,\alpha,1,2\text{-}\eta\text{:}3,4,5,6\text{-}\eta\text{-C}_6\text{H}_5\text{C(Ph)C=CH}_2\}]$  (**11**).

|                  |                   |                     |                   |
|------------------|-------------------|---------------------|-------------------|
| Rh1–C1           | 2.138(4)          | Rh1–C2              | 2.171(4)          |
| Rh1–C7           | 2.112(5)          | Rh1–C8              | 2.128(5)          |
| Rh1–(C15 to C19) | 2.197(5)–2.267(5) | Rh2–C3              | 2.211(5)          |
| Rh2–C4           | 2.117(5)          | Rh2–C5              | 2.095(5)          |
| Rh2–C6           | 2.166(5)          | Rh2–(C20 to C24)    | 2.191(5)–2.278(5) |
| C1–C2            | 1.423(6)          | C1–C6               | 1.482(6)          |
| C1–C7            | 1.440(6)          | C2–C3               | 1.478(7)          |
| C3–C4            | 1.422(7)          | C4–C5               | 1.429(7)          |
| C5–C6            | 1.426(7)          | C7–C8               | 1.432(7)          |
| C7–C9            | 1.490(6)          | C9 to C14–C9 to C14 | 1.369(9)–1.396(7) |
| C2–C1–C6         | 115.7(4)          | C2–C1–C7            | 118.2(4)          |
| C6–C1–C7         | 126.0(4)          | C1–C2–C3            | 112.4(4)          |
| C2–C3–C4         | 122.3(4)          | C3–C4–C5            | 114.9(4)          |
| C4–C5–C6         | 114.9(4)          | C5–C6–C1            | 119.9(4)          |
| C1–C7–C8         | 114.7(4)          | C1–C7–C9            | 120.9(4)          |
| C8–C7–C9         | 124.3(4)          |                     |                   |

The molecules consist of a 1-( $\eta^5\text{-C}_5\text{H}_5$ )-1-rhodaindenyl bicyclic ring system, which is  $\pi$ -coordinated through its  $\text{RhC}_4$  ring to another  $[\text{Rh}(\eta\text{-C}_5\text{H}_5)]$  group in an  $\eta^5$  fashion. The rhodium atom Rh1 is displaced from the plane of the four carbon atoms of the five-membered metallacyclic ring, in the direction away from Rh2. The six-membered ring of the rhodaindenyl is nearly planar (root mean-square deviation from the best plane 0.01–0.02 Å). Selected bond lengths and angles are presented in Table 6.

**Photochemical reaction of  $[\text{Rh}(\eta\text{-C}_5\text{H}_5)(\text{C}_2\text{H}_4)_2]$  (**5**) with 1,3,5-triisopropenylbenzene:** A 1:1.2 mixture of **5** and 1,3,5-triisopropenylbenzene in pentane/diethyl ether was irradiated at  $-5^\circ\text{C}$  for 36 hours. The major substances isolated by chromatographic workup were the unreacted starting materials (40% **5** and 50% of the benzene derivative). Five additional product fractions were obtained by column chromatography. The first four fractions only contained trace amounts of material. The last fraction gave the orange dirhodium complex  $[\text{Rh}(\eta\text{-C}_5\text{H}_5)]_2(\mu\text{-}\beta,\alpha,1,2\text{-}\eta\text{:}\beta',\alpha')$ ,

Figure 5. Molecular structure of the complex  $[\text{Rh}(\eta\text{-C}_5\text{H}_5)\{1\text{-}3,8,9\text{-}\eta\text{-}[1\text{-}(\eta\text{-C}_5\text{H}_5)]\text{-}3\text{-Ph-1-rhodaindenyl}\}]$  (**12a**).

coupling of several resonances to both rhodium nuclei. The carbon atoms C2 and C9, simultaneously  $\sigma$ -bonded to one rhodium atom and  $\pi$ -bonded to the other, show the largest couplings to  $^{103}\text{Rh}$  ( $J(\text{Rh},\text{C}) \approx 44$  and 15 Hz). In a similar manner to that of the proton H2, their resonances are also shifted to low field ( $\delta = 153$ ).

Separation of **12b** from the major product **9c** by column chromatography was incomplete. After repeated crystallization of the raw product only small amounts of pure **12b** were finally obtained. The composition of this complex was established by mass spectroscopy and a single-crystal X-ray structure analysis. Because of the poor crystallinity of the material, the accuracy of this structure is limited. To provide a better definition of the geometry of **12**, an X-ray structure analysis was also carried out with a single crystal of **12a**. Views of the molecules are shown in Figures 5 and 6.

The asymmetric unit of **12b** contains two independent molecules which differ only by the rotational orientation of the cyclopentadienyl rings on both rhodium atoms. If the phenyl and methyl substituents are disregarded, the molecular structure of **12a** is also very similar.

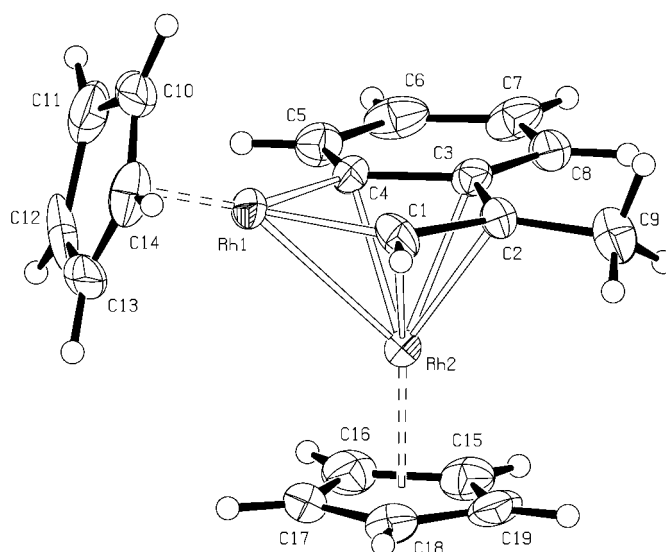
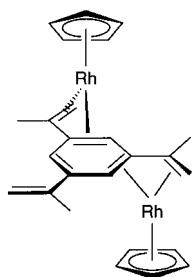
Figure 6. Molecular structure of the complex  $[\text{Rh}(\eta\text{-C}_5\text{H}_5)\{1\text{-}3,8,9\text{-}\eta\text{-}[1\text{-}(\eta\text{-C}_5\text{H}_5)]\text{-}3\text{-CH}_3\text{-1-rhodaindenyl}\}]$  (**12b**).

Table 6. Selected bond lengths [ $\text{\AA}$ ] and angles [ $^\circ$ ] for the complexes  $[\text{Rh}(\eta\text{-C}_5\text{H}_5)[1\text{-}3,8,9\text{-}\eta\text{-}\{1\text{-}(\eta\text{-C}_5\text{H}_5)\}\text{-}3\text{-R}^1\text{-}1\text{-rhodaindenyl}]]$  **12a** and **12b**.

|   | <b>12a</b>        | <b>12b</b> <sup>[a]</sup>               |
|---|-------------------|---|
| Rh1–Rh2/Rh3–Rh4                           | 2.6299(3)         | 2.633(2)/2.616(2)                       |
| Rh1–C1/Rh3–C20                            | 1.989(2)          | 1.955(13)/1.957(12)                     |
| Rh1–C4/Rh3–C23                            | 2.003(2)          | 2.015(11)/2.016(12)                     |
| Rh1/Rh3–C(C <sub>5</sub> H <sub>5</sub> ) | 2.190(2)–2.273(2) | 2.156(13)–2.276(11)/2.191(13)–2.256(13) |
| Rh2–C1/Rh4–C20                            | 2.192(2)          | 2.179(11)/2.188(12)                     |
| Rh2–C2/Rh4–C21                            | 2.175(2)          | 2.142(11)/2.164(11)                     |
| Rh2–C3/Rh4–C22                            | 2.226(2)          | 2.214(11)/2.192(11)                     |
| Rh2–C4/Rh4–C23                            | 2.249(2)          | 2.235(11)/2.227(12)                     |
| Rh2/Rh4–C(C <sub>5</sub> H <sub>5</sub> ) | 2.183(2)–2.235(2) | 2.177(12)–2.212(12)/2.147(14)–2.228(11) |
| C1–C2/C20–C21                             | 1.427(3)          | 1.44(2)/1.43(2)                         |
| C2–C3/C21–C22                             | 1.447(3)          | 1.44(2)/1.44(2)                         |
| C3–C4/C22–C23                             | 1.452(3)          | 1.46(2)/1.45(2)                         |
| C3–C8/C22–C27                             | 1.430(3)          | 1.41(2)/1.48(2)                         |
| C4–C5/C23–C24                             | 1.435(3)          | 1.42(2)/1.42(2)                         |
| C5–C6/C24–C25                             | 1.368(4)          | 1.37(2)/1.36(2)                         |
| C6–C7/C25–C26                             | 1.419(4)          | 1.43(2)/1.41(2)                         |
| C7–C8/C26–C27                             | 1.365(3)          | 1.36(2)/1.36(2)                         |
| C1–Rh1–C4/C20–Rh3–C23                     | 78.94(9)          | 78.9(5)/79.4(5)                         |
| Rh1–C1–C2/Rh3–C20–C21                     | 118.9(2)          | 120.5(9)/120(1)                         |
| C1–C2–C3/C20–C21–C22                      | 112.4(2)          | 111(1)/110(1)                           |
| C2–C3–C4/C21–C22–C23                      | 112.2(2)          | 112.7(9)/114(1)                         |
| C3–C4–Rh1/C22–C23–Rh3                     | 117.4(2)          | 116.5(8)/115.3(9)                       |

[a] Two independent molecules.

**13**

4,3- $\eta$ -1,3,5-triisopropenylbenzene)] (**13**) in 14 % yield after recrystallization.

Complex **13** was characterized by mass and NMR spectroscopic methods. In the  $^1\text{H}$  and  $^{13}\text{C}$  NMR spectra, there are two closely spaced but still clearly resolved doublet resonances for the two  $\{\text{Rh}(\eta\text{-C}_5\text{H}_5)\}$  groups. The rest of the spectra are also consistent with

the fairly low symmetry of the molecule. The three ring protons of the triisopropenylbenzene ligand resonate at  $\delta = 7.10$ , 2.82, and 2.00. The last two resonances show evident coupling to one  $^{103}\text{Rh}$  nucleus. There are three groups of  $^1\text{H}$  resonances from the methylene groups ( $\delta = 5.16$ , 5.97; 2.58, 2.64; 0.56, 0.74) that are spread over a large area of the spectrum.

Treatment of **13** with  $[\text{Co}(\eta\text{-C}_5\text{H}_5)(\eta\text{-C}_6\text{Me}_6)]^{[7c]}$  in THF, or UV irradiation in *n*-pentane in the presence of **5** did not lead to the addition of a  $\{\text{M}(\eta\text{-C}_5\text{H}_5)\}$  group ( $\text{M} = \text{Co}, \text{Rh}$ ) to the noncoordinated isopropenyl substituent. Rapid decomposition of **13** was observed above  $50^\circ\text{C}$ .

## Discussion

Since it was first reported in 1980, the Jonas reagent  $[\text{Co}(\eta\text{-C}_5\text{H}_5)(\text{C}_2\text{H}_4)_2]^{[7]}$  has become firmly established as an easy-to-handle yet highly reactive source of the  $\{\text{Co}(\eta\text{-C}_5\text{H}_5)\}$  fragment.<sup>[8,9]</sup> In contrast, its rhodium analogue  $[\text{Rh}(\eta\text{-C}_5\text{H}_5)(\text{C}_2\text{H}_4)_2]$  (**5**) is thermally quite stable and kinetically rather inert towards substitution of the ethylene ligands under

thermal conditions.<sup>[10]</sup> However, UV photolysis of **5** was shown to lead to extrusion of ethylene and formation of the highly reactive species  $[\text{Rh}(\eta\text{-C}_5\text{H}_5)(\text{C}_2\text{H}_4)]$  and/or  $[\text{Rh}(\eta\text{-C}_5\text{H}_5)(\text{C}_2\text{H}_4)(\text{solvent})]$ , which in turn could be easily converted into a variety of complexes of the type  $[\text{Rh}(\eta\text{-C}_5\text{H}_5)(\text{C}_2\text{H}_4)_2\text{-}n\text{L}_n]$  ( $n = 1, 2$ ).<sup>[11]</sup> Although the photolytic reactions of **5** were reported to proceed quite cleanly when carried out on a small scale, UV irradiation of solutions containing higher concentrations of **5** (typically around 0.01M) quickly leads to a strong darkening, which effectively quenches the radiation and progressively slows down the formation of the photo-products. Part of this effect, which is probably caused by the formation of minute

amounts of polynuclear rhodium complexes, could be overcome by the use of a falling film photoreactor. Nevertheless, reaction of **5** becomes very slow after a few hours and the reactions typically had to be stopped at  $\approx 40\text{--}50\%$  conversion.

The photoreactions of **5** with alkenylbenzenes follow two channels: formation of  $\pi$  complexes and C–H activation of the organic substrate, as discussed in more detail below.

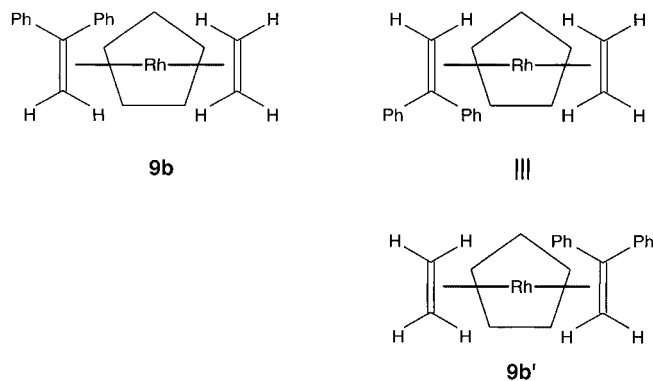
**The mononuclear complexes  $[\text{Rh}(\eta\text{-C}_5\text{H}_5)(\eta\text{-C}_2\text{H}_4)(\eta^2\text{-alkenylbenzene})]$  (**9a–c**) and  $[\text{Rh}(\eta\text{-C}_5\text{H}_5)(\eta^4\text{-alkenylbenzene})]$  (**10**):** The ethylene  $\eta^2$ -alkenylbenzene complexes **9** represent the primary product of the reaction between **5** and the alkenylbenzene. The latter is bonded to the metal exclusively through the  $\pi$  system of the alkenyl substituent, rather than through the phenyl group. Complexes of the type  $[\text{Rh}(\eta\text{-C}_5\text{H}_5)(\eta\text{-C}_2\text{H}_4)(\eta^2\text{-olefin})]$  are rare. Only two examples,  $[\text{Rh}(\eta\text{-C}_5\text{H}_5)(\eta\text{-C}_2\text{H}_4)(\eta\text{-C}_2\text{F}_4)]^{[12]}$  and  $[\text{Rh}(\eta\text{-C}_5\text{H}_5)(\eta\text{-C}_2\text{H}_4)(9,10\text{-}\eta\text{-phenanthrene})]$  (**14**),<sup>[13]</sup> have been structurally characterized.

The *cis* configuration of the stilbene ligand in **9a** is not surprising. Photoisomerization of *trans*- into *cis*-stilbene and vice versa is a well-known process, which will generate a high stationary concentration of the *cis* isomer during the reaction.<sup>[14]</sup> For steric reasons, the *cis*-stilbene complex **9a** should be preferred to the *trans* isomer, which was indeed not observed.

The temperature-dependent NMR spectra of **9a–c** are accounted for by dynamic processes that involve “in-place” rotation of the two olefin ligands.<sup>[15]</sup> In complex **9a**, rotation of the  $\eta^2$ -ethylene leads to exchange of the *endo* and *exo* hydrogen atoms of its two chemically equivalent methylene groups. The onset of this process gives rise to the broad

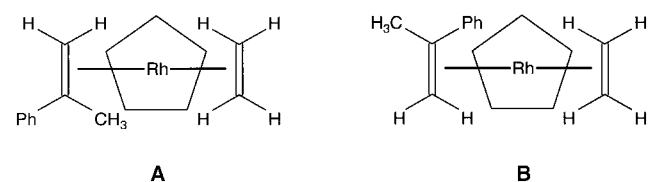
appearance of these resonances in the room temperature spectra.

In the low-temperature spectra of the less symmetric **9b**, every olefinic proton of the ethylene and 1,1-diphenylethylene ligands appears as a well-resolved separate resonance, which is in agreement with a rigid chiral structure on the NMR ( $T_2$ ) timescale (two enantiomers **9b** and **9b'**). Rotation



of the ligands leads to racemization and causes significant broadening of these resonances at room temperature. In contrast to **9a**, which effectively has a mirror plane bisecting the two olefins, the dynamic process in **9b** also affects the carbon resonances of the ethylene ligand, which are sharp at low temperature and broaden on warming.

The spectra of **9c** are more complicated. Two chiral diastereomers are present in solution, as shown by the presence of two resonances for  $\{\text{Rh}(\eta\text{-C}_5\text{H}_5)\}$  both in the proton and carbon spectra. On steric grounds, conformation **A** with the methyl group of the  $\alpha$ -methylstyrene ligand in the *endo* position is tentatively assigned to the more abundant species (60%). Most likely, **A** and **B** are racemic mixtures.



A complete assignment of the low-temperature proton and carbon spectra is given in Tables 1 and 2. Clearly, the observed coalescence of the  $\{\text{Rh}(\eta\text{-C}_5\text{H}_5)\}$  proton resonances at 27 °C requires fast (on the NMR timescale) rotation of at least the  $\alpha$ -methylstyrene ligand, thus interconverting the diastereomers **A** and **B**. Racemization is not effected by a mere in-place rotation of the  $\eta^2$ -olefins.

The molecular structures of **9a** and **9b** can be derived from that of the bis-ethylene complex **5**, which has a distorted trigonal coordination of the rhodium atom.<sup>[16]</sup> They are similar to that of the  $\eta^2$ -phenanthrene complex **14**.<sup>[13]</sup> Consistently, of the two  $\eta^2$ -coordinated C=C bonds of the olefin ligands, the one in the  $\eta^2$ -ethylene is somewhat shorter (by 0.02–0.03 Å). Steric repulsions of the phenyl rings in **9a** are minimized by a small degree of torsion (6.6°) around C1–C2, and by a larger twist of the phenyl ring planes with respect to each other and

to the olefinic plane. A similar geometry has been reported for the  $\eta^2$  *cis*-stilbene ligand in  $[\text{Re}(\eta\text{-C}_5\text{H}_5)\{(\text{Ph}_2\text{P})_2\text{CH}_2\text{-CH}_2\}[\eta^2\text{-(Z)-stilbene}]]$ .<sup>[17]</sup>

In the 1,1-diphenylethylene complex **9b**, the steric situation is less favorable, because of the *endo* position with respect to the  $\eta^2$ -ethylene of one of the phenyl groups. Consequently, bonding of the two olefinic termini of the diphenylethylene to the rhodium is more asymmetric, with the Rh1–C2 bond being the longest rhodium olefin–carbon bond in the molecule. Interestingly, the angles enclosed by the lines connecting the centers of the two olefin ligands to the rhodium atom are quite similar in **9a** and **9b**.

Loss of ethylene from **9b** generates the  $\eta^4$ -1,1-diphenylethylene rhodium complex **10**. The  $\eta^2$ -coordinated phenyl ring has now apparently lost most of its aromaticity, as shown by the strong alternation of short (1.35/1.36 Å) and long (1.43–1.44 Å) C–C bonds in its noncoordinated “diene” part. The essentially equal C–C bond lengths within the  $\eta^4$ -diene unit are indicative of extensive delocalization within this substructure.

In the literature, there are many examples of complexes of conjugated dienes with  $\{\text{Rh}(\eta\text{-C}_5\text{R}_5)\}$  fragments. To our knowledge, the complexes **10** and **13** are the first in which one of the C–C bonds of the  $\eta^4$ -diene is a part of an aromatic ring system. No complex of the type  $[\text{Rh}(\eta\text{-C}_5\text{H}_5)(\beta,\alpha,1,2\text{-}\eta\text{-alkenylbenzene})]$  was formed with stilbene as a ligand. Starting from complex **9a** with a  $\eta^2$ -(Z)-stilbene ligand, a phenyl substituent would attain the *endo* position on C $\beta$ ; this is clearly a sterically very unfavorable situation.

The localization of bonds within the  $\eta^4$ -alkenylbenzene in **10** promotes addition of a second  $\{\text{Rh}(\eta\text{-C}_5\text{H}_5)\}$  fragment to the six-membered ring that is already partially coordinated to the metal. On the grounds of the eighteen valence electron rule, no metal–metal bonding is required in an  $\eta^4:\eta^4$  complex. An *anti* position of the two metals, which minimizes steric repulsions, is therefore preferred. In complex **11**, the separation of the  $\mu$ -alkenylbenzene ligand into two  $\eta^4$ -diene units is clearly reflected in the C–C bond lengths. The C1–C6 and C2–C3 bonds, which join the two  $\eta^4$ -diene moieties, are considerably longer (1.48 Å) than those within the “diene” units (1.42–1.44 Å). Unlike in complex **10**, the six-membered ring in complex **11** is not planar, but strongly folded (34°) along the transannular vector C3...C6. This can be attributed to the generally observed torsion of the “outer” C–C bonds in  $\eta^4$ -coordinated dienes, to minimize repulsion between the *endo* substituents at the termini, and to optimize  $\pi$  overlap with the metal orbitals.

A number of mononuclear<sup>[18–20]</sup> and dinuclear<sup>[19]</sup> iron–carbonyl complexes analogous to **10** and **11** have been reported. The structural<sup>[18, 21]</sup> and spectroscopic<sup>[19]</sup> data as well as chemical reactivity<sup>[19]</sup> of all these complexes consistently indicate a loss of aromatic character of the coordinated arene.

The only product that could be isolated from the reaction of **5** and 1,3,6-triisopropenylbenzene was the dinuclear complex **13**. It is reasonable to assume that this compound is formed via the intermediates  $[\text{Rh}(\eta\text{-C}_5\text{H}_5)(\beta,\alpha\text{-}\eta\text{-triisopropenylbenzene})(\text{C}_2\text{H}_4)]$  (**15**) and  $[\text{Rh}(\eta\text{-C}_5\text{H}_5)(\beta,\alpha,1,2\text{-}\eta\text{-triisopropenylbenzene})]$  (**16**), which would be close analogues of the complexes **9** and **10**. Once formed, the mononuclear complex

**16** is expected to be more reactive than the free triisopropenylbenzene ligand towards further addition of  $\{\text{Rh}(\eta\text{-C}_5\text{H}_5)\}$  fragments, on account of the greater localization of bonds within the arene ring which is already partially coordinated to the metal. This could be an explanation as to why complex **16** was not observed. Complex **13** has all the spectroscopic properties expected for a  $\eta^4$ -1,3-diene complex. In principle, there could be two isomers of **13**, with the two  $\{\text{Rh}(\eta^5\text{-C}_5\text{H}_5)\}$  groups in a *syn* or an *anti* arrangement with respect to the bridging arene ring. However, only one isomer was observed. For steric reasons, we believe the  $\{\text{Rh}(\eta^5\text{-C}_5\text{H}_5)\}$  groups to prefer the *anti* arrangement, in accord with the crystallographically established structure of  $[\{\text{Fe}(\text{CO})_3\}_2(\mu\text{-}p\text{-divinylbenzene})]$ .<sup>[22]</sup>

Further addition of a third  $\{\text{M}(\eta\text{-C}_5\text{H}_5)\}$  fragment ( $\text{M} = \text{Co}, \text{Rh}$ ) to the dinuclear complex **13** would have to occur in a position *syn* to one of the  $\{\text{Rh}(\eta\text{-C}_5\text{H}_5)\}$  moieties. This is clearly unfavorable and the likely cause for the reaction to stop at the dinuclear stage.

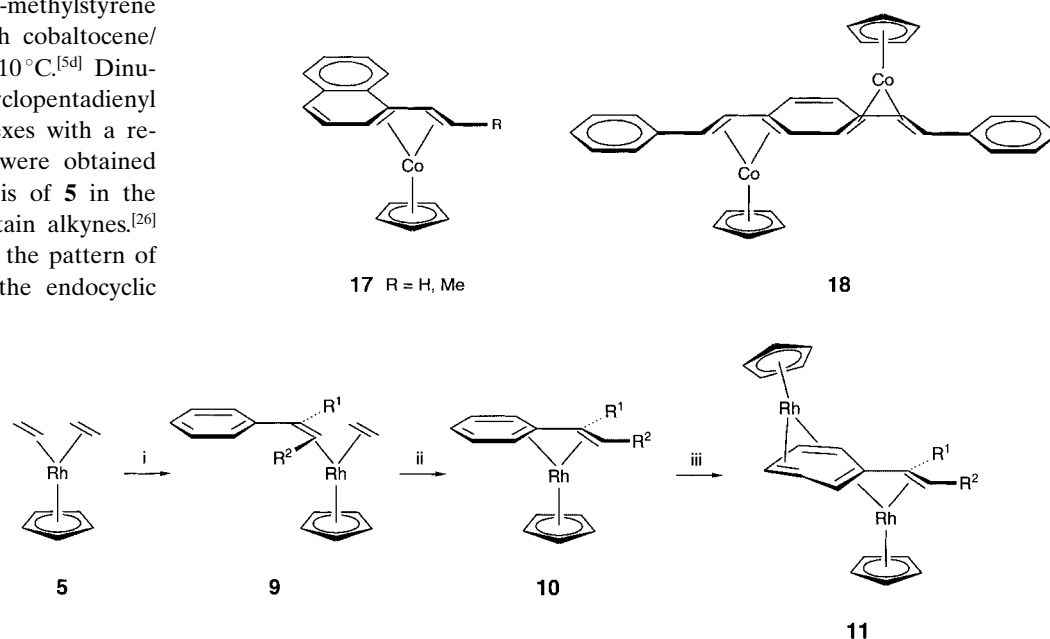
**The rhodaindenyl complexes  $[\text{Rh}(\eta\text{-C}_5\text{H}_5)(1\text{-rhodaindenyl})]$  (**12a**, **12b**):** The rhodaindenyl ligands are the products of a twofold activation of the C–H bond in the corresponding alkenylbenzenes at the  $\beta$  and *ortho* positions. No attempts were made to establish the fate of the two hydrogen atoms that are eliminated from the product.

Analogous metallaindenyl complexes have been reported with the metal ligand fragments  $\{\text{M}(\eta\text{-C}_5\text{H}_5)\}$  ( $\text{M} = \text{Co}, \text{Ir}$ )<sup>[5d, 23]</sup> and  $\{\text{M}(\text{CO})_3\}$  ( $\text{M} = \text{Fe}, \text{Os}$ ).<sup>[24]</sup> In thermal reactions, the complexes  $[\text{Co}(\eta\text{-C}_5\text{Me}_4\text{R})\{1\text{-}3,8,9\text{-}\eta\text{-}\{1\text{-}(\eta\text{-C}_5\text{Me}_4\text{R})\}\text{-}3\text{-CH}_3\text{-}1\text{-cobaltaindenyl}\}]$  can be obtained in  $\approx 30\%$  yield from  $\alpha$ -methylstyrene and  $[\text{Co}(\eta\text{-C}_5\text{Me}_4\text{R})(\text{C}_2\text{H}_4)_2]$  ( $\text{R} = \text{Me}, \text{Et}$ ).<sup>[25]</sup> In marked contrast,  $[\text{Co}(\eta\text{-C}_5\text{H}_5)(\text{C}_2\text{H}_4)_2]$  and this styrene derivative gave  $[\{\text{Co}(\eta\text{-C}_5\text{H}_5)\}_3\{\mu_3\text{-C}_6\text{H}_5\text{C}(\text{Me})=\text{CH}_2\}]$ , a facial arene complex of type **1**, in very high yield.<sup>[5a, 5b]</sup> The complex  $[\text{Co}(\eta\text{-C}_5\text{H}_5)\{1\text{-}3,8,9\text{-}\eta\text{-}\{1\text{-}(\eta\text{-C}_5\text{H}_5)\}\text{-}3\text{-CH}_3\text{-}1\text{-cobaltaindenyl}\}]$  was only formed in a very small yield when  $\alpha$ -methylstyrene was treated with cobaltocene/potassium at  $-10^\circ\text{C}$ .<sup>[5d]</sup> Dinuclear rhodacyclopentadienyl (rhodol) complexes with a related structure were obtained by the photolysis of **5** in the presence of certain alkynes.<sup>[26]</sup> As indicated by the pattern of the lengths of the endocyclic

C–C bonds, the  $\pi$  system is fairly localized in the six-membered ring of the rhodaindenyl ligand in **12**, which is similar to the situation in the  $\eta^4$ -1,1-diphenylethylene complex **10**. The structural features of the rhodaindenyl ligand compare well with those reported for the few other complexes of analogous composition.<sup>[5d, 25, 27]</sup>

**Formation of the title complexes and significance for the syntheses of the cluster complexes  $[\{\text{M}(\eta\text{-C}_5\text{H}_5)\}_3(\mu_3\text{-arene})]$ :** Evidently, the mononuclear and dinuclear complexes  $[\text{Rh}(\eta\text{-C}_5\text{H}_5)(\eta\text{-C}_2\text{H}_4)(\eta^2\text{-alkenylbenzene})]$  (**9**),  $[\text{Rh}(\eta\text{-C}_5\text{H}_5)(\beta,\alpha,1,2\text{-}\eta\text{-alkenylbenzene})]$  (**10**), and  $[\{\text{Rh}(\eta\text{-C}_5\text{H}_5)\}_2(\mu\text{-}\beta,\alpha,1,2\text{-}\eta\text{-}3,4,5,6\text{-}\eta\text{-alkenylbenzene})]$  (**11**) represent subsequent substitution steps of the ethylene ligands in **5** by the alkenylbenzene ligand (Scheme 3). Formation of  $[\{\text{Rh}(\eta\text{-C}_5\text{H}_5)\}_2(\mu\text{-}\beta,\alpha,1,2\text{-}\eta\text{-}\beta',\alpha',4,3\text{-}\eta\text{-}1,3,5\text{-triisopropenylbenzene})]$  **13** follows a similar pathway. However, the rhodaindenyl complexes **12** result from a second reaction channel, which involves activation of two C–H bonds.<sup>[2a]</sup> Based on our preparative results, we assume that this reaction starts from the  $\eta^2$ -alkenylbenzene complexes **9**, because these are the only ones in the series **9**, **10**, and **11** which could be transformed into **12**. Although activation of vinylic C–H bonds does not necessarily require prior  $\pi$  coordination of the olefin,<sup>[28]</sup> the sequence  $\pi$  coordination  $\rightarrow$  C–H activation has been amply demonstrated in the literature.<sup>[29]</sup>

In earlier work, we proposed that the addition of  $\{\text{Co}(\eta\text{-C}_5\text{H}_5)\}$  fragments to alkenylbenzenes follows a pathway initially analogous to Scheme 3.<sup>[6]</sup> In the  $\{(d^9\text{-M})(\eta\text{-C}_5\text{H}_5)\}$  series, the rhodium complexes **9** and **10** are the first direct analogues of the mononuclear intermediates **6** and **7** (Scheme 2). With the preparation and characterization of complexes such as  $[\text{Co}(\eta\text{-C}_5\text{H}_5)(\text{vinyl}n\text{aphthalene})]$  (**17**) and  $[\{\text{Co}(\eta\text{-C}_5\text{H}_5)\}_2(\mu\text{-distyrylbenzene})]$  (**18**), we were able to demonstrate the feasibility of  $\beta,\alpha,1,2\text{-}\eta^4$  coordination of alkenylarenes to cyclopentadienylcobalt fragments.<sup>[5d, 6]</sup> These

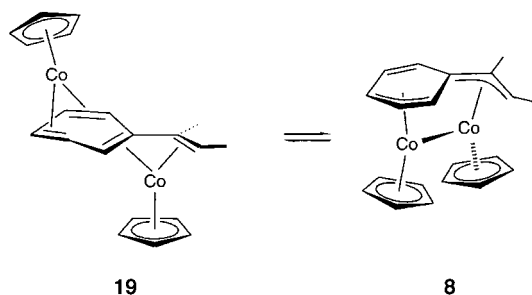


Scheme 3. i)  $\text{PhC}(\text{R}^1)=\text{C}(\text{H})\text{R}^2$ ,  $h\nu$ ,  $-\text{C}_2\text{H}_4$ ; ii)  $h\nu$ ,  $-\text{C}_2\text{H}_4$ ; iii) **5**,  $h\nu$ ,  $-2\text{C}_2\text{H}_4$ .



complexes are more labile than their rhodium counterparts, and indeed no  $\{\text{Co}(\eta\text{-C}_5\text{H}_5)\}$  complex of a simple alkenylbenzene has yet been isolated.

When a trinuclear arene-capped cluster is to be formed, the metals must be brought together on the same face of the ligand at some stage, most likely already in a dinuclear intermediate. Evidently, this happens in the cobalt series, where  $\mu_3$ -arene cluster complexes **1** are frequently formed, sometimes even in quantitative yield. Dinuclear complexes [*anti*- $\{\text{M}(\eta\text{-C}_5\text{H}_5)\}_2(\mu\text{-}\eta^4\text{:}\eta^4\text{-alkenylbenzene})$ ] with the two metals on opposite faces of the arene are likely to be formed with both  $\text{M} = \text{Co}$  and  $\text{M} = \text{Rh}$ . For the formation of trinuclear cluster complexes [ $\{\text{M}(\eta\text{-C}_5\text{H}_5)\}_3(\mu_3\text{-arene})$ ] these are dead ends. The rhodium system becomes trapped at this point (for example, complex **11**) on account of the stability of the Rh–diene bonds. For  $\text{M} = \text{Co}$ , we propose an equilibrium between two types of dinuclear complexes, with an *anti* (complex **19**) and a *syn* arrangement, respectively, of the metals. For the latter, structure **8** has been proposed, which gains stability in a sterically less favorable situation by a Co–Co bond.<sup>[6]</sup> A structure analogous to **4** (Scheme 1) is an alternative possibility.



If  $\{\text{Co}(\eta\text{-C}_5\text{H}_5)\}$  is compared to its isolobal counterpart  $\{\text{Fe}(\text{CO})_3\}$ , we note that metal–metal bonding is much less preferred between the carbonyl metal fragments.<sup>[30]</sup> This could explain the kinetic stability of the complexes [*anti*- $\{\text{Fe}(\text{CO})_3\}_2(\mu\text{-}\eta^4\text{:}\eta^4\text{-alkenylbenzene})$ ],<sup>[19]</sup> and also helps to explain the lack of an iron complex<sup>[31]</sup> in the series [ $\{\text{d}^8\text{-M}(\text{CO})_3\}_3(\mu_3\text{-arene})$ ], which is well documented for  $\text{M} = \text{Ru}$  and  $\text{Os}$ .<sup>[32]</sup>

## Experimental Section

**General procedures:** All operations were carried out under an atmosphere of purified nitrogen or argon (BASFR3–11 catalyst) by means of Schlenk techniques. Solvents were dried by conventional methods. Alumina (Macherey–Nagel, neutral), used as a stationary phase for column chromatography, was heated to 250–300 °C under vacuum for 24 h and then stored under nitrogen. An all-quartz Normag falling-film UV reactor equipped with a Heraeus high-pressure mercury lamp (power rating: 150, 180 or 700 W) was used for photochemical reactions. Complex **5** was prepared according to the literature procedure.<sup>[10]</sup> NMR spectra were obtained on a Bruker Avance DRX200 instrument (200.1 MHz for  $^1\text{H}$ , 50.3 MHz for  $^{13}\text{C}$ ).  $^1\text{H}$  and  $^{13}\text{C}$  chemical shifts are reported with respect to  $\text{SiMe}_4$  and were determined by reference to internal  $\text{SiMe}_4$  or residual solvent peaks. Assignment of the carbon resonances was routinely corroborated by DEPT (135°) spectra. Mass spectra were recorded in the electron impact ionization mode (EI) at 70 eV on VG 7070H and Finnigan MAT8400 spectrometers. Elemental analyses were performed in-house with a Heraeus CHN–O–Rapid instrument.

**Reaction of **5** with *trans*-stilbene:** In the falling-film photoreactor, a solution of *trans*-stilbene (740 mg, 4.1 mmol) in diethyl ether (80 mL) was mixed with **5** (820 mg, 3.6 mmol) in *n*-pentane (350 mL). Irradiation was carried out at 0 °C with a 150 W mercury lamp (6 h). Solvent was removed from the orange solution to give an oily residue, which was redissolved in a little *n*-hexane and purified by chromatography at –20 °C ( $\text{Al}_2\text{O}_3$ , 5%  $\text{H}_2\text{O}$ , 2.5 × 17 cm, *n*-hexane). A mixture of stilbene and **5** was eluted first as a yellow fraction. A second orange band gave a mixture of stilbene and  $[\text{Rh}(\eta\text{-C}_5\text{H}_5)(\text{C}_2\text{H}_4)(\eta^2\text{-}(Z)\text{-stilbene})]$  (**9a**) after removal of solvent under vacuum. Repeated recrystallization from *n*-pentane gave **9a** (30 mg, 2% yield) as orange needles.

**Complex **9a**:** EI-MS (%):  $m/z$ : 376 (4) [ $\text{M}^+$ ], 349 (21) [ $\text{C}_5\text{H}_5\text{RhL}^+ + \text{H}$ ], 348 (100) [ $\text{C}_5\text{H}_5\text{RhL}^+$ ], 180 (13) [ $\text{L}^+$ ], 168 (74) [ $\text{C}_5\text{H}_5\text{Rh}^+$ ], 103 (8) [ $\text{Rh}^+$ ];  $\text{L} = \text{stilbene}$ ; elemental analysis calcd (%) for  $\text{C}_{21}\text{H}_{21}\text{Rh}$  (376.30): C 67.02, H 5.62; found: C 67.12, H 5.85.

**Reaction of **5** with 1,1-diphenylethylene in *n*-hexane:** A mixture of **5** (950 mg, 4.2 mmol) and 1,1-diphenylethylene (780 mg, 4.3 mmol) in *n*-hexane (400 mL) was irradiated with a 150 W mercury lamp at –5 °C for 30 h. The solvent was evaporated under vacuum from the resulting red-brown solution, and the residue was purified by chromatography at –20 °C ( $\text{Al}_2\text{O}_3$ , 2.5 × 23 cm). With *n*-hexane as an eluent, a mixture of **5** and 1,1-diphenylethylene (300 mg after evaporation of solvent) was washed from the column, followed by a red and a yellow band. The solvent was evaporated under reduced pressure from the product fractions. Recrystallization of the red product from *n*-pentane gave microcrystals of  $[\text{Rh}(\eta\text{-C}_5\text{H}_5)\{\beta,\alpha,1,2\text{-}\eta^4\text{-(}\alpha\text{-phenylstyrene)}\}]$  (**10**). Yield: 60 mg (4%). The trace amount of yellow product was identified by mass spectroscopy as  $[\text{Rh}(\eta\text{-C}_5\text{H}_5)(\eta\text{-C}_2\text{H}_4)(\eta^2\text{-1,1-diphenylethylene})]$  (**9b**). A fourth red-brown fraction was obtained with *n*-hexane/diethyl ether (30:1, v:v), which after removal of solvent under vacuum gave dark microcrystals (95 mg, 9% yield) of  $[\text{Rh}(\eta\text{-C}_5\text{H}_5)\{1\text{-3,8,9-}\eta\text{-[1-(}\eta\text{-C}_5\text{H}_5)\text{-3-Ph-1-rhodaindenyl}]\}]$  (**12a**).

**Complex **10**:**  $^1\text{H}$  NMR ( $\text{C}_6\text{D}_6$ ):  $\delta$  = 0.59 (“”, 1H;  $\text{H}\beta_{\text{endo}}$ ), 2.73 (s, 1H;  $\text{H}\beta_{\text{exo}}$ ), 3.11 (d, 1H;  $\eta^2$ -phenyl-H2), 4.72 (d,  $J(\text{Rh,H}) = 0.9$  Hz, 5H;  $\text{C}_5\text{H}_5$ ), 6.69 (m, 2H; phenyl-H), 7.10 (m, 4H; phenyl-H), 7.59 (d,  $\eta^2$ -phenyl-H6), 7.71 (m, 2H; phenyl-H);  $^{13}\text{C}\{^1\text{H}\}$  NMR ( $\text{C}_6\text{D}_6$ ):  $\delta$  = 34.0 (d,  $J(\text{Rh,C}) = 16.5$  Hz,  $\text{CH}_2$ ), 59.3 (d,  $J(\text{Rh,C}) = 11.5$  Hz,  $\eta^2$ -phenyl-C2), 82.7 (d,  $J(\text{Rh,C}) = 5.2$  Hz,  $\text{C}_5\text{H}_5$ ), 83.9 (d,  $J(\text{Rh,C}) = 6.0$  Hz,  $\eta^2$ -phenyl- $\text{C}_{\text{ipso}}/\text{Ca}$ ), 84.8 (d,  $J(\text{Rh,C}) = 6.0$  Hz,  $\eta^2$ -phenyl- $\text{C}_{\text{ipso}}/\text{Ca}$ ), 121.5 (s, phenyl-CH), 125.6 (s, phenyl-CH), 127.1 (s, phenyl-CH), 127.2 (s, phenyl-CH), 128.6 (s, phenyl-CH), 132.4 (s, phenyl-CH), 138.4 (s, phenyl-CH), 141.0 (s, phenyl- $\text{C}_{\text{ipso}}$ ); EI-MS (%):  $m/z$ : 348 (20) [ $\text{M}^+$ ], 347 (7) [ $\text{M}^+ - \text{H}$ ], 181 (15) [ $\text{L}^+ + \text{H}$ ], 180 (100) [ $\text{L}^+$ ], 179 (50) [ $\text{L}^+ - \text{H}$ ], 178 (41) [ $\text{L}^+ - 2\text{H}$ ], 168 (48) [ $\text{C}_5\text{H}_5\text{Rh}^+$ ], 165 (51) [ $\text{L}^+ - \text{CH}_3$ ], 92 (26) [ $\text{C}_7\text{H}_8^+$ ], 91 (29) [ $\text{C}_7\text{H}_7^+$ ];  $\text{L} = \text{diphenylethylene}$ ; elemental analysis calcd (%) for  $\text{C}_{19}\text{H}_{17}\text{Rh}$  (348.25): C 65.53, H 4.92; found: C 65.40, H 5.23.

**Complex **12a**:**  $^1\text{H}$  NMR ( $\text{C}_6\text{D}_6$ ):  $\delta$  = 4.74 (d,  $J(\text{Rh,H}) = 1.1$  Hz, 5H;  $\text{C}_5\text{H}_5$ ), 5.28 (d,  $J(\text{Rh,H}) = 0.7$  Hz, 5H;  $\text{C}_5\text{H}_5$ ), 6.65 (m, 1H;  $\text{C}_6\text{H}_4\text{-H4/H5}$ ), 6.81 (m, 1H;  $\text{C}_6\text{H}_4\text{-H4/H5}$ ), 7.18 (d, 1H; phenyl), 7.57 (dd, 4H; phenyl), 7.70 (d, 1H;  $\text{C}_6\text{H}_4\text{-H3/H6}$ ), 8.01 (m, 1H;  $\text{C}_6\text{H}_4\text{-H3/H6}$ ), 8.17 (d,  $J(\text{Rh,H}) = 0.7$  Hz, 1H;  $\text{H}\beta$ );  $^{13}\text{C}\{^1\text{H}\}$  NMR ( $\text{C}_6\text{D}_6$ ):  $\delta$  = 82.4 (d,  $J(\text{Rh,C}) = 6.8$  Hz,  $\text{C}_2\text{H}_3$ ), 83.3 (d,  $J(\text{Rh,C}) = 3.9$  Hz,  $\text{C}_5\text{H}_5$ ), 112.9 (dd,  $J(\text{Rh,C}) = 4.9/2.6$  Hz,  $\text{C}_6\text{H}_4\text{-C/Ca}$ ), 116.6 (dd,  $J(\text{Rh,C}) = 4.8/2.9$  Hz,  $\text{C}_6\text{H}_4\text{-C/Ca}$ ), 121.72 (s,  $\text{C}_6\text{H}_4\text{-CH}$ ), 126.7 (s,  $\text{C}_6\text{H}_4\text{-CH/phenyl-CH}$ ), 127.1 (s,  $\text{C}_6\text{H}_4\text{-CH/phenyl-CH}$ ), 128.2 (s,  $\text{C}_6\text{H}_4\text{-CH/phenyl-CH}$ ), 130.6 (s,  $\text{C}_6\text{H}_4\text{-CH/phenyl-CH}$ ), 140.7 (s, phenyl-C), 149.5 (s,  $\text{C}_6\text{H}_4\text{-CH}$ ), 153.2 (dd,  $J(\text{Rh,C}) = 43.1/14.8$  Hz,  $\text{C}\beta$ ), 153.5 (dd,  $J(\text{Rh,C}) = 44.3/14.8$  Hz,  $\text{C}_6\text{H}_4\text{-C2}$ ); EI-MS (%):  $m/z$ : 515 (23) [ $\text{M}^+ + \text{H}$ ], 514 (100) [ $\text{M}^+$ ], 449 (11) [ $\text{M}^+ - \text{C}_5\text{H}_5$ ], 233 (48) [ $(\text{C}_5\text{H}_5)_2\text{Rh}^+$ ], 168 (5) [ $\text{C}_5\text{H}_5\text{Rh}^+$ ]; elemental analysis calcd (%) for  $\text{C}_{24}\text{H}_{20}\text{Rh}_2$  (514.23): C 56.05, H 3.92; found: C 55.56, H 4.07.

**Reaction of **5** with 1,1-diphenylethylene in *n*-hexane/diethyl ether/acetonitrile:** A mixture of **5** (820 mg, 3.6 mmol) and 1,1-diphenylethylene (690 mg, 3.8 mmol) in a mixture of *n*-hexane (350 mL), diethyl ether (50 mL), and acetonitrile (50 mL) was irradiated with a 700 W mercury lamp at –8 °C for 8 h. The solvent was evaporated under vacuum from the resulting red-brown solution and the residue was purified by chromatography at –20 °C ( $\text{Al}_2\text{O}_3$ , 2.5 × 27 cm). Three fractions were washed from the column with *n*-hexane to give 300 mg of a mixture of **5** and 1,1-diphenylethylene, traces of **10** and yellow microcrystals of  $[\text{Rh}(\eta\text{-C}_5\text{H}_5)(\eta\text{-C}_2\text{H}_4)(\eta^2\text{-1,1-diphenylethylene})]$  (**9b**) (90 mg, 7% after recrystallization from *n*-pentane). A blue fraction was obtained with *n*-hexane/toluene (10:1, v:v). Removal of

solvent under vacuum and double recrystallization of the residue from *n*-pentane gave black microcrystals of  $[\text{Rh}(\eta\text{-C}_5\text{H}_5)_2]_2(\mu\text{-}\beta,\alpha,1,2\text{-}\eta\text{-}3,4,5,6\text{-}\eta\text{-}(\alpha\text{-phenylstyrene}))$  (**11**, 60 mg, 9.5% yield).

**Complex 9b**: EI-MS (%):  $m/z$ : 348 (15)  $[M^+ - \text{C}_2\text{H}_4]$ , 180 (60) [diphenylethylene<sup>+</sup>], 168 (100)  $[\text{C}_5\text{H}_5\text{Rh}^+]$ ; elemental analysis calcd (%) for  $\text{C}_{21}\text{H}_{21}\text{Rh}$  (376.30): C 67.02, H 5.62; found: C 66.92, H 5.65.

**Complex 11**:  $^1\text{H}$  NMR ( $\text{C}_6\text{D}_6$ ):  $\delta$  = 0.34 (m, 1H;  $\text{H}\beta_{\text{endo}}$ ), 2.53 (brm, 2H;  $\eta^4\text{-}\eta^4\text{-phenyl-H/H}\beta_{\text{exo}}$ ), 3.85 ("t", 1H;  $\eta^4\text{-}\eta^4\text{-phenyl-H3}$ ), 3.92 ("d", 1H;  $\eta^4\text{-}\eta^4\text{-phenyl-H6}$ ), 4.86 (d,  $J(\text{Rh,H})$  = 0.9 Hz, 5H;  $\text{C}_5\text{H}_5$ ), 5.04 (d,  $J(\text{Rh,H})$  = 0.9 Hz, 5H;  $\text{C}_5\text{H}_5$ ), 5.58 (m, 1H;  $\eta^4\text{-}\eta^4\text{-phenyl-H4/H5}$ ), 6.04 (m, 1H;  $\eta^4\text{-}\eta^4\text{-phenyl-H4/H5}$ ), 7.14 (m, 3H; phenyl-H), 7.71 (d, 1H; phenyl-H), 7.73 ("t", 1H; phenyl-H);  $^{13}\text{C}\{^1\text{H}\}$  NMR ( $\text{C}_6\text{D}_6$ ):  $\delta$  = 32.3 (d,  $J(\text{Rh,H})$  = 18.4 Hz,  $\text{CH}_2$ ), 51.4 (d,  $J(\text{Rh,C})$  = 16.2 Hz,  $\eta^4\text{-}\eta^4\text{-phenyl-C3/C6}$ ), 60.6 (d,  $J(\text{Rh,C})$  = 13.0 Hz,  $\eta^4\text{-}\eta^4\text{-phenyl-C2}$ ), 62.3 (d,  $J(\text{Rh,C})$  = 16.2 Hz,  $\eta^4\text{-}\eta^4\text{-phenyl-C3/C6}$ ), 76.5 (d,  $J(\text{Rh,C})$  = 6.5 Hz,  $\eta^4\text{-}\eta^4\text{-phenyl-C4/C5}$ ), 80.1 (d,  $J(\text{Rh,C})$  = 6.5 Hz,  $\eta^4\text{-}\eta^4\text{-phenyl-C4/C5}$ ), 82.7 (d,  $J(\text{Rh,C})$  = 5.4 Hz,  $\text{C}_5\text{H}_5$ ), 84.8 (d,  $J(\text{Rh,C})$  = 4.3 Hz,  $\text{C}_5\text{H}_5$ ), 92.9 (d,  $J(\text{Rh,C})$  = 9.5 Hz,  $\eta^4\text{-}\eta^4\text{-phenyl-C}_{\text{ipso}}/\text{Ca}$ ), 101.5 (d,  $J(\text{Rh,C})$  = 6.4 Hz,  $\eta^4\text{-}\eta^4\text{-phenyl-C}_{\text{ipso}}/\text{Ca}$ ), 127.1 (s, phenyl-CH), 127.7 (s, phenyl-CH), 132.1 (s, phenyl-CH), 140.5 (s, phenyl-C); EI-MS (%):  $m/z$ : 516 (37)  $[M^+]$ , 514 (72)  $[M^+ - 2\text{H}]$ , 349 (12)  $[(\text{C}_5\text{H}_5\text{RhL})^+ + \text{H}]$ , 348 (72)  $[\text{C}_5\text{H}_5\text{RhL}^+]$ , 233 (95)  $[(\text{C}_5\text{H}_5)_2\text{Rh}^+]$ , 181 (13)  $[\text{L}^+ + \text{H}]$ , 180 (95)  $[\text{L}^+]$ , 179 (50)  $[\text{L}^+ - \text{H}]$ , 178 (42)  $[\text{L}^+ - 2\text{H}]$ , 168 (100)  $[\text{C}_5\text{H}_5\text{Rh}^+]$ , 165 (82), 103 (17)  $[\text{Rh}^+]$ ; L = diphenylethylene; elemental analysis calcd (%) for  $\text{C}_{24}\text{H}_{22}\text{Rh}_2$  (516.25): C 55.83, H 4.29; found: C 56.31, H 4.09.

**Reaction of  $[\text{Rh}(\eta\text{-C}_5\text{H}_5)]_2(\mu\text{-}\beta,\alpha,1,2\text{-}\eta\text{-}(\alpha\text{-phenylstyrene}))$  (**10**) with **5****: A mixture of **10** (55 mg, 0.16 mmol) and **5** (40 mg, 0.18 mmol) in diethyl ether (50 mL) was irradiated with a 150 W mercury lamp at  $-20^\circ\text{C}$  for 6 h. The products were worked up by column chromatography ( $\text{Al}_2\text{O}_3$ , 5%  $\text{H}_2\text{O}$ ,  $2 \times 16$  cm). *n*-Hexane was used to wash unreacted **5** ( $\approx 10$  mg) and **10** ( $\approx 10$  mg) from the column. The main product,  $[\text{Rh}(\eta\text{-C}_5\text{H}_5)]_2(\mu\text{-}\beta,\alpha,1,2\text{-}\eta\text{-}3,4,5,6\text{-}\eta\text{-}(\alpha\text{-phenylstyrene}))$  (**11**), was eluted with *n*-hexane/toluene (10:1, v:v). Recrystallization from *n*-pentane gave a 19 mg yield of dark crystalline **11** (46% yield based on converted **10**).

**Reaction of **5** with  $\alpha$ -methylstyrene**: A solution of  $\alpha$ -methylstyrene (680 mg, 5.7 mmol) in diethyl ether (100 mL) was added to a solution of **5** (940 mg, 4.2 mmol) in *n*-hexane (300 mL). The mixture was irradiated with a 150 W mercury lamp at  $0^\circ\text{C}$  for 40 h. The resulting red solution was filtered, the solvent was removed under reduced pressure, and the oily residue was dried under vacuum (room temperature, 10 h). Chromatographic separation of the products was carried out on alumina at  $-20^\circ\text{C}$  (5%  $\text{H}_2\text{O}$ ,  $3.5 \times 24$  cm). *n*-Hexane, was used to wash **5** (500 mg) from the column as a yellow band. A second orange fraction gave 190 mg (14% yield) of **9c** as a yellow solid after removal of solvent under vacuum and recrystallization from *n*-pentane. A red-brown fraction was obtained on further elution with *n*-hexane/diethyl ether (10:1, v:v). Removal of solvent under vacuum gave 40 mg (4%) of **12b** as a brown solid.

**Complex 9c**: EI-MS (%):  $m/z$ : 314 (1.5)  $[M^+]$ , 287 (17)  $[(\text{C}_5\text{H}_5\text{RhL})^+ + \text{H}]$ , 286 (88)  $[\text{C}_5\text{H}_5\text{RhL}^+]$ , 169 (13)  $[(\text{C}_5\text{H}_5\text{Rh})^+ + \text{H}]$ , 168 (100)  $[\text{C}_5\text{H}_5\text{Rh}^+]$ , 103 (14)  $[\text{Rh}^+]$ ; L =  $\alpha$ -methylstyrene.

**Complex 12b**: EI-MS (%):  $m/z$ : 453 (8)  $[M^+ + \text{H}]$ , 452 (47)  $[M^+]$ , 233 (44)  $[\text{C}_5\text{H}_5\text{Rh}^+]$ .

**Reaction of **5** with 1,3,5-triisopropenylbenzene**: A solution of **5** (970 mg, 4.3 mmol) and 1,3,5-triisopropenylbenzene (990 mg, 5.0 mmol) in *n*-pentane (400 mL) was irradiated with a

180 W mercury lamp at  $-5^\circ\text{C}$  for 36 h. The solvent was removed under vacuum and the residue was purified by chromatography at  $-20^\circ\text{C}$  ( $\text{Al}_2\text{O}_3$ ,  $2.5 \times 22$  cm, *n*-hexane). Six yellow bands and one orange band were eluted from the column. The first yellow fraction contained unreacted **5** ( $\approx 40\%$ ) and 1,3,5-triisopropenylbenzene. After removal of solvent, the other yellow fractions gave only minute amounts of material, which were not examined further. Evaporation of the solvent under vacuum from the orange band left an orange solid that was repeatedly recrystallized from *n*-hexane/toluene (10:1, v:v) to give orange  $[\text{Rh}(\eta\text{-C}_5\text{H}_5)]_2(\mu\text{-}\beta,\alpha,1,2\text{-}\eta\text{-}\beta',\alpha',4,3\text{-}\eta\text{-}1,3,5\text{-triisopropenylbenzene})$  (**13**, 70 mg, 14% yield based on converted **5**).

**Complex 13**:  $^1\text{H}$  NMR ( $\text{C}_6\text{D}_6$ ):  $\delta$  = 0.56 (m, 1H;  $\text{H}\beta_{\text{endo}}$ ), 0.74 ("t", 1H;  $\text{H}\beta_{\text{endo}}$ ), 2.00 (d,  $J(\text{Rh,H})$  = 2.0 Hz, 1H; arene-H2/H4), 2.08 (d, 3H;  $\text{CH}_3$ ), 2.24 (s, 3H;  $\text{CH}_3$ ), 2.33 (s, 3H;  $\text{CH}_3$ ), 2.58 (m, 1H;  $\text{H}\beta_{\text{exo}}$ ), 2.64 (m, 1H;  $\text{H}\beta_{\text{exo}}$ ), 2.82 (d,  $J(\text{Rh,H})$  = 2.0 Hz, 1H; arene-H2/H4), 4.87 (d,  $J(\text{Rh,H})$  = 1.0 Hz, 5H;  $\text{C}_5\text{H}_5$ ), 4.88 (d,  $J(\text{Rh,H})$  = 1.0 Hz, 5H;  $\text{C}_5\text{H}_5$ ), 5.16 (m, 1H; alkene-H), 5.97 (m, 1H; alkene-H), 7.10 (s, 1H; arene-H);  $^{13}\text{C}\{^1\text{H}\}$  NMR ( $\text{C}_6\text{D}_6$ ):  $\delta$  = 20.2 (s,  $\text{CH}_3$ ), 21.0 (s, 2  $\text{CH}_3$ ), 35.3 (d,  $J(\text{Rh,C})$  = 17.5 Hz, alkene- $\text{CH}_2$ ), 36.2 (d,  $J(\text{Rh,C})$  = 17.5 Hz, alkene- $\text{CH}_2$ ), 48.0 (d,  $J(\text{Rh,C})$  = 14.0 Hz, arene-CH), 50.5 (d,  $J(\text{Rh,C})$  = 14.0 Hz, arene-CH), 84.0 (d,  $J(\text{Rh,C})$  = 5.4 Hz,  $\text{C}_5\text{H}_5$ ), 84.1 (d,  $J(\text{Rh,C})$  = 5.4 Hz,  $\text{C}_5\text{H}_5$ ), 86.1 (d,  $J(\text{Rh,C})$  = 8.5 Hz, arene-C1/C3/Ca), 88.1 (d,  $J(\text{Rh,C})$  = 7.5 Hz, arene-C1/C3/Ca), 89.8 (d,  $J(\text{Rh,C})$  = 7.5 Hz, arene-C1/C3/Ca), 113.7 (s, free alkene- $\text{CH}_2$ ), 116.2 (s, arene-C6), 142.7 (s, alkene-Ca), 147.4 (s, arene-C5); EI-MS (%):  $m/z$ : 534 (37)  $[M^+]$ , 533 (6)  $[M^+ - \text{H}]$ , 532 (38)  $[M^+ - 2\text{H}]$ , 366 (7)  $[\text{C}_5\text{H}_5\text{RhL}^+]$ , 233 (50)  $[(\text{C}_5\text{H}_5)_2\text{Rh}^+]$ , 168 (37)  $[\text{C}_5\text{H}_5\text{Rh}^+]$ ; L = 1,3,5-triisopropenylbenzene.

**Crystal structure determinations**. Single crystals of the complexes **9a**, **9b**, **10**, **11**, **12a**, and **12b** were obtained from solutions in *n*-pentane. Crystal data are compiled in Tables 7 and 8. Intensity data were collected at low temperature on a Siemens-Stoe AED2 four-circle diffractometer and on a Bruker AXS SMART CCD diffractometer. A semiempirical absorption correction was applied. The structures were solved by direct methods, and refined by full-matrix least-squares based on  $F^2$  and by using all measured unique reflections. All non-hydrogen atoms were given anisotropic displacement parameters. Some of the hydrogen atoms were localized in

Table 7. Details of the crystal structure determinations of the complexes **9a**, **9b**, and **10**.

|   | <b>9a</b>                                      | <b>9b</b>                             | <b>10</b>                             |
|---|--|---------------------------------------|---------------------------------------|
| formula   | $\text{C}_{21}\text{H}_{21}\text{Rh}$          | $\text{C}_{21}\text{H}_{21}\text{Rh}$ | $\text{C}_{19}\text{H}_{17}\text{Rh}$ |
| crystal system  | monoclinic                                     | monoclinic                            | orthorhombic                          |
| space group   | $P2_1/n$                                       | $P2_1/n$                              | $Fdd2$                                |
| $a$ [Å]   | 12.773(6)                                      | 8.5219(5)                             | 14.9005(7)                            |
| $b$ [Å]   | 7.263(4)                                       | 8.1632(5)                             | 53.065(3)                             |
| $c$ [Å]   | 17.711(9)                                      | 23.7016(15)                           | 7.0950(3)                             |
| $\alpha$ [°]  | 90   | 90                                    | 90                                    |
| $\beta$ [°]   | 92.86(3)                                       | 94.980(1)                             | 90                                    |
| $\gamma$ [°]  | 90   | 90                                    | 90                                    |
| $V$ [Å <sup>3</sup> ]                                 | 1641.0(15)                                     | 1642.6(2)                             | 5609.9(4)                             |
| $Z$   | 4  | 4                                     | 16                                    |
| $M_r$   | 376.30   | 376.30                                | 348.25                                |
| $\rho_{\text{calcd}}$ [Mg m <sup>-3</sup> ]           | 1.523  | 1.522                                 | 1.649                                 |
| $F_{000}$   | 768  | 768                                   | 2816                                  |
| $\mu(\text{MoK}\alpha)$ [mm <sup>-1</sup> ]           | 1.035  | 1.034                                 | 1.203                                 |
| $\lambda$ [Å]   | MoK $\alpha$ , graphite monochromated, 0.71073 |                                       |                                       |
| $T$ [K]   | 203  | 173                                   | 173                                   |
| $2\theta$ range [°]                                   | 3–60   | 3–56.6                                | 3–56                                  |
| $hkl$ range   | –17/17, 0/10, 0/24                             | –11/11, 0/10, 0/31                    | 0/19, 0/70, –9/8                      |
| measured reflections                                  | 4782   | 11 255                                | 19 155                                |
| unique reflections ( $R_{\text{int}}$ )               | 4782   | 4005 (0.035)                          | 3181 (0.027)                          |
| observed reflections [ $I \geq 2\sigma(I)$ ]          | 3971   | 3648                                  | 3075                                  |
| parameters refined                                    | 284  | 225                                   | 192                                   |
| $R$ [ $I \geq 2\sigma(I)$ ]                           | 0.028  | 0.034                                 | 0.033                                 |
| wR2 (all data)  | 0.069  | 0.090                                 | 0.083                                 |
| $A$ , $B^{[a]}$                                       | 0.0323, 0.48                                   | 0.0362, 3.45                          | 0.0595, 0.67                          |
| $P^{[a]}$   |  | $\max(F_o^2, 0) + 2F_o^2/3$           |                                       |
| GoF   | 1.03   | 1.173                                 | 1.115                                 |
| largest difference peak and hole [e Å <sup>-3</sup> ] | 0.43/–0.58                                     | 1.25/–0.80                            | 3.95/–0.39                            |

[a]  $w = 1/[\sigma^2(F) + (A \cdot P)^2 + (B \cdot P)]$ .

Table 8. Details of the crystal structure determinations of complexes **11**, **12a**, and **12b**.

|  | <b>11</b>                                       | <b>12a</b>  | <b>12b</b>                                      |
|--|---|---|---|
| formula  | C <sub>24</sub> H <sub>22</sub> Rh <sub>2</sub> | C <sub>24</sub> H <sub>20</sub> Rh <sub>2</sub>   | C <sub>19</sub> H <sub>18</sub> Rh <sub>2</sub> |
| crystal system   | triclinic                                       | triclinic   | monoclinic                                      |
| space group  | $P\bar{1}$                                      | $P\bar{1}$  | $P2_1/c$  |
| <i>a</i> [Å]   | 9.159(5)  | 9.2226(8)   | 9.399(5)  |
| <i>b</i> [Å]   | 10.852(5)                                       | 9.6651(8)   | 14.942(7)                                       |
| <i>c</i> [Å]   | 11.181(6)                                       | 11.8252(10)   | 22.731(11)                                      |
| $\alpha$ [°]   | 114.61(2)                                       | 111.264(2)  | 90  |
| $\beta$ [°]  | 96.78(2)  | 98.349(2)   | 98.55(3)  |
| $\gamma$ [°]   | 107.15(2)                                       | 106.515(2)  | 90  |
| <i>V</i> [Å <sup>3</sup> ]                                 | 927.6(8)  | 904.7(1)  | 3157(3)   |
| <i>Z</i>   | 2   | 2   | 8   |
| <i>M</i> <sub>r</sub>                                      | 516.25  | 514.23  | 452.16  |
| $\rho_{\text{calcd}}$ [Mg m <sup>-3</sup> ]                | 1.848   | 1.888   | 1.903   |
| <i>F</i> <sub>000</sub>                                    | 512   | 508   | 1776  |
| $\mu(\text{Mo K}\alpha)$ [mm <sup>-1</sup> ]               | 1.783   | 1.828   | 2.08  |
| $\lambda$ [Å]  | Mo K $\alpha$ , graphite monochromated, 0.71073 |   |   |
| <i>T</i> [K]   | 203   | 173   | 203   |
| 2 $\theta$ range [°]                                       | 4–56  | 4–56  | 3–54  |
| <i>hkl</i> range   | –12/11, –14/13, 0/14                            | –12/12, –12/12, 0/15  | –12/11, 0/19, 0/29                              |
| measured reflections                                       | 4476  | 12187   | 6844  |
| unique reflections ( <i>R</i> <sub>int</sub> )             | 4476  | 4388 (0.025)  | 6844  |
| observed reflections [ <i>I</i> ≥ 2 $\sigma$ ( <i>I</i> )] | 3328  | 3892  | 5574  |
| parameters refined   | 323   | 315   | 393   |
| <i>R</i> [ <i>I</i> ≥ 2 $\sigma$ ( <i>I</i> )]             | 0.037   | 0.023   | 0.064   |
| w <i>R</i> 2 (all data)                                    | 0.082   | 0.062   | 0.181   |
| <i>A</i> , <i>B</i> <sup>[a]</sup>                         | 0.033, 0.33                                     | 0.0444, 0.0   | 0.0335, 78.35                                   |
| <i>P</i> <sup>[a]</sup>                                    |   | max( <i>F</i> <sub>o</sub> <sup>2</sup> , 0) + 2 <i>F</i> <sub>c</sub> <sup>2</sup> /3) |   |
| GoF  | 1.032   | 1.006   | 1.206   |
| largest difference peak and hole [e Å <sup>-3</sup> ]      | 0.48/–0.79                                      | 0.71/–0.62  | 1.41/–1.62                                      |

[a]  $w = 1/[\sigma^2(F) + (A \cdot P)^2 + (B \cdot P)]$ .

difference Fourier syntheses and refined isotropically. The remaining hydrogen atoms were placed in calculated positions.<sup>[33]</sup> The calculations were performed with the programs SHELXS-86 and SHELXL-97.<sup>[34]</sup> Graphical representations were drawn with PLATON.<sup>[35]</sup> Anisotropic displacement ellipsoids are scaled to 40 % probability.

## Acknowledgements

This work was supported by the Deutsche Forschungsgemeinschaft and the Fonds der Chemischen Industrie. Donations of valuable chemicals by DEGUSSA AG Hanau are gratefully acknowledged.

- Review articles: a) H. Wadepohl, *Angew. Chem.* **1992**, 104, 253; *Angew. Chem. Int. Ed. Engl.* **1992**, 31, 247; b) H. Wadepohl, S. Gebert, *Coord. Chem. Rev.* **1995**, 143, 535.
- a) H. Wadepohl, A. Metz, in *Metal Clusters in Chemistry, Vol. 1* (Eds.: P. Braunstein, L. A. Oro, P. R. Raithby), Wiley-VCH, **1999**, Chapter 1.15; b) H. Wadepohl, in *Physical Organometallic Chemistry Vol. 3* (Ed.: M. Gielen), Wiley, **2001**, in print.
- J. Müller, P. Escarpa Gaede, K. Qiao, *Angew. Chem.* **1993**, 105, 1809; *Angew. Chem. Int. Ed. Engl.* **1993**, 32, 1697.
- J. Müller, P. Escarpa Gaede, K. Qiao, *J. Organomet. Chem.* **1994**, 480, 213.
- a) H. Wadepohl, K. Büchner, H. Pritzkow, *Angew. Chem.* **1987**, 99, 1294; *Angew. Chem. Int. Ed. Engl.* **1987**, 26, 1259; b) H. Wadepohl, K. Büchner, M. Herrmann, H. Pritzkow, *Organometallics* **1991**, 10, 861; c) H. Wadepohl, T. Borchert, K. Büchner, H. Pritzkow, *Chem. Ber.* **1993**, 126, 1615; d) H. Wadepohl, T. Borchert, K. Büchner, M. Herrmann, F.-J. Paffen, H. Pritzkow, *Organometallics* **1995**, 14, 3817; e) H. Wadepohl, T. Borchert, H. Pritzkow, *J. Organomet. Chem.* **1996**, 516, 187; f) H. Wadepohl, M. J. Calhorda, M. Herrmann, C. Jost, P. E. M. Lopes, H. Pritzkow, *Organometallics* **1996**, 15, 5622; g) H. Wadepohl, K. Büchner, M. Herrmann, A. Metz, H. Pritzkow, *J. Organomet. Chem.* **1998**, 571, 267; h) H. Wadepohl, K. Büchner, M. Herrmann, H. Pritzkow, *J. Organomet. Chem.* **1998**, 573, 22.
- H. Wadepohl, K. Büchner, H. Pritzkow, *Organometallics* **1989**, 8, 2745.
- K. Jonas, C. Krüger, *Angew. Chem.* **1980**, 92, 513; *Angew. Chem. Int. Ed. Engl.* **1980**, 92, 513; b) K. Jonas, *Adv. Organomet. Chem.* **1981**, 19, 97; c) K. Jonas, E. Deffense, D. Habermann, *Angew. Chem.* **1983**, 95, 729 [*Angew. Chem. Suppl.* **1983**, 1005]; *Angew. Chem. Int. Ed. Engl.* **1983**, 22, 716.
- K. Jonas, *J. Organomet. Chem.* **1990**, 400, 165.
- H. Wadepohl, *Comments Inorg. Chem.* **1994**, 15, 369.
- R. Cramer, *Inorg. Chem.* **1962**, 1, 722; R. Cramer, *J. Am. Chem. Soc.* **1967**, 89, 4621; R. Cramer, *J. Am. Chem. Soc.* **1972**, 94, 5681.
- a) D. M. Haddleton, R. N. Perutz, *J. Chem. Soc. Chem. Commun.* **1985**, 1372; b) S. T. Belt, D. M. Haddleton, R. N. Perutz, B. P. H. Smith, A. J. Dixon, *J. Chem. Soc. Chem. Commun.* **1987**, 1347; c) S. T. Belt, S. B. Duckett, D. M. Haddleton, R. N. Perutz, *Organometallics* **1989**, 8, 748; d) T. W. Bell, D. M. Haddleton, A. McCamley, M. G. Partridge, R. N. Perutz, *J. Am. Chem. Soc.* **1990**, 112, 9212.
- L. J. Guggenberger, R. Cramer, *J. Am. Chem. Soc.* **1972**, 94, 3779.
- J. Müller, C. Hirsch, K. Qiao, Kwang Ha, *Z. Anorg. Allg. Chem.* **1996**, 622, 1441.
- C. D. Berweger, W. F. van Gunsteren, F. Müller-Plathe, *Angew. Chem.* **1999**, 111, 2771; *Angew. Chem. Int. Ed.* **1999**, 38, 2609; and references therein.
- a) R. Cramer, *J. Am. Chem. Soc.* **1964**, 86, 217; b) R. Cramer, J. D. Cline, J. D. Roberts, *J. Am. Chem. Soc.* **1969**, 91, 2519; c) R. Cramer, J. Mrowca, *Inorg. Chim. Acta* **1971**, 5, 528.
- K. A. Klandermaun, *Diss. Abstr.* **1965**, 25, 6253.
- C. Carfagna, N. Carr, R. J. Deeth, S. J. Dossett, M. Green, M. F. Mahon, C. Vaughan, *J. Chem. Soc. Dalton Trans.* **1996**, 415.
- a) W. A. Herrmann, J. Weichmann, B. Balbach, M. L. Ziegler, *J. Organomet. Chem.* **1982**, 231, C69; b) V. G. Adrianov, Yu. T. Struchkov, G. M. Babakhina, I. I. Kritskaya, D. N. Kravtsov, *Izv. Akad. Nauk SSSR Ser. Khim.* **1985**, 590.
- R. Victor, R. Ben-Shoshan, S. Sarel, *Tetrahedron Lett.* **1970**, 49, 4253; *J. Chem. Soc. Chem. Commun.* **1970**, 1680; *J. Chem. Soc. Chem. Commun.* **1971**, 1241; *J. Org. Chem.* **1972**, 37, 1930.
- H. Fleckner, F.-W. Grevels, D. Hess, *J. Am. Chem. Soc.* **1984**, 106, 2027.
- F. H. Herbstein, M. G. Reisner, *Acta Crystallogr. Sect. B* **1977**, 33, 3304.
- a) T. A. Manuel, S. L. Stafford, F. G. A. Stone, *J. Am. Chem. Soc.* **1961**, 83, 3597; b) R. E. Davis, R. J. Pettit, *J. Am. Chem. Soc.* **1970**, 92, 716.
- a) P. Binger, T. R. Martin, R. Benn, A. Ruffinska, G. Schroth, *Z. Naturforsch. Teil B* **1984**, 39, 993; b) W. D. McGhee, R. G. Bergman, *J. Am. Chem. Soc.* **1988**, 110, 4246.
- a) W. Hübel, E. H. Braye, *J. Inorg. Nucl. Chem.* **1959**, 10, 250; b) R. E. Davis, B. L. Barnett, R. G. Amiet, W. Merk, J. S. McKennis, R. Pettit, *J. Am. Chem. Soc.* **1974**, 96, 7108; c) R. Victor, R. Ben-Shoshan, *J. Chem. Soc. Chem. Commun.* **1974**, 93; d) Y. Degreève, J. Meunier-Piret, M. van Meerssche, P. Piret, *Acta Crystallogr. Sect. B* **1967**, B23,

- 119; e) P. J. Harris, J. A. K. Howard, S. A. R. Knox, R. P. Phillips, F. G. A. Stone, P. Woodward, *J. Chem. Soc. Dalton Trans.* **1976**, 377.
- [25] A. Metz, Ph.D. Dissertation, Heidelberg **1999**; H. Wadepohl, A. Metz, H. Pritzkow, unpublished results.
- [26] a) S. A. Gardner, P. S. Andrews, M. D. Rausch, *Inorg. Chem.* **1973**, *12*, 2396; b) J. Müller, T. Akhnoukh, P. Escarpa Gaede, A. Guo, P. Moran, K. Qiao, *J. Organomet. Chem.* **1997**, *541*, 207.
- [27] W. D. McGhee, R. G. Bergmann, *J. Am. Chem. Soc.* **1988**, *110*, 4246.
- [28] J. Silvestre, M. J. Calhorda, R. Hoffmann, P. O. Stoutland, R. G. Bergman, *Organometallics* **1986**, *5*, 1841.
- [29] a) W. D. Jones, F. J. Feher, *Acc. Chem. Res.* **1989**, *22*, 91, and references therein; b) A. E. Shilov, G. B. Shul'pin, *Chem. Rev.* **1997**, *97*, 2879, and references therein.
- [30] M. Elia, M. M. L. Chen, D. M. P. Mingos, R. Hoffmann, *Inorg. Chem.* **1976**, *15*, 1148.
- [31] H. Wadepohl, S. Gebert, H. Pritzkow, *J. Organomet. Chem.* **2000**, *614–615*, 158.
- [32] a) M. P. Gomez-Sal, B. F. G. Johnson, J. Lewis, P. R. Raithby, A. H. Wright, *J. Chem. Soc. Chem. Commun.* **1985**, 1682; b) B. F. G. Johnson, J. Lewis, M. Martinelli, A. H. Wright, D. Braga, F. Grepioni, *J. Chem. Soc. Chem. Commun.* **1990**, 364.
- [33] CCDC-167233 (**9a**), CCDC-167234 (**9b**), CCDC-167235 (**10**), CCDC-167236 (**11**), CCDC-167237 (**12a**) and CCDC-167238 (**12b**) contain the supplementary crystallographic data for this paper. These data can be obtained free of charge via [www.ccdc.cam.ac.uk/conts/retrieving.html](http://www.ccdc.cam.ac.uk/conts/retrieving.html) (or from the Cambridge Crystallographic Data Centre, 12 Union Road, Cambridge CB2 1EZ, UK; fax: (+44) 1223-336-033; or e-mail: [deposit@ccdc.cam.ac.uk](mailto:deposit@ccdc.cam.ac.uk)).
- [34] SHELXS-86: G. M. Sheldrick, *Acta Crystallogr. Sect. A* **1990**, *46*, 467; G. M. Sheldrick, SHELXL-97, Universität Göttingen (Germany), **1997**.
- [35] A. L. Spek, *PLATON*, Utrecht University, Utrecht (The Netherlands), **2001**; A. L. Spek, *Acta Crystallogr. Sect. A* **1990**, *46*, C31.

Received: July 16, 2001 [F3420]